

## Wilson loops in three dimensions

Kevin Cahill

*Lyman Laboratory of Physics, Harvard University, Cambridge, Massachusetts 02138,  
Division de Physique Théorique, Institut de Physique Nucléaire, Université de Paris-Sud, 91406 Orsay, France,  
and Department of Physics and Astronomy, University of New Mexico, Albuquerque, New Mexico 87131\**

Sudhakar Prasad

*Center for Advanced Studies and Department of Physics and Astronomy, University of New Mexico, Albuquerque, New Mexico 87131*

(Received 12 September 1988; revised manuscript received 1 May 1989)

For a pure gauge theory in three dimensions with a compact, semisimple gauge group, we derive a formula for Creutz ratios of Wilson loops that is valid in the continuum theory to fourth order in the coupling constant. For  $SU(2)_3$ , we compare this perturbative formula, corrected for periodic boundary conditions, with lattice Creutz ratios that we have measured both in compact simulations guided by Wilson's or Manton's action and in noncompact simulations guided by the Yang-Mills action. The noncompact simulations show no evidence of quark confinement. We also present a critique of compact lattice methods and discuss the renormalization of both compact and noncompact simulations.

### I. INTRODUCTION

In the strong-coupling limit, quark confinement is a nearly universal property of Wilson's lattice gauge theory,<sup>1</sup> holding for almost all gauge groups and space-time dimensions. In this sense, confinement is built into Wilson's method. In the weak-coupling limit, lattice simulations of QCD are *believed* to converge to QCD itself. Hence the open questions: Is the confinement seen in lattice simulations of QCD at moderate coupling<sup>2,3</sup> a relic of the built-in confinement of the strong-coupling limit or a reflection of a true property of QCD? Does pure QCD confine quarks—or are light quarks an essential part of the confinement mechanism, as recently suggested by Gribov?<sup>4</sup>

It is not possible to answer these questions by performing the simulations at the very small values of the coupling constant  $g$  at which they are believed to be correct, because the lattice spacing  $a$  shrinks with  $g$  like  $e^{-8\pi^2/11g^2} \approx e^{-7/g^2}$ . So to study confinement, which is characterized by a fixed distance scale, near  $g=0$  would require a nearly infinite computer.

As a way of determining whether pure QCD confines quarks and of answering other questions in field theory, Patrascioiu, Seiler, Stamatescu, Zwanziger, Yotsuyanagi, and Nešić<sup>5-8</sup> and our group<sup>9-13</sup> have developed Monte Carlo methods that directly approximate the ratios of Euclidean path integrals that occur in QCD and in other continuum gauge theories. These methods may be called "noncompact" because their basic variables are the fields themselves rather than the elements of a gauge group as in Wilson's "compact" method. Patrascioiu, Seiler, and Stamatescu use a discrete form of the continuum action; we interpolate the fields throughout space-time and use the continuum action itself. They fix the gauge, we do not. Both noncompact methods may be closer to the continuum theory than Wilson's method, and neither has

confinement trivially built in.

To provide a standard against which to compare the results of compact and noncompact simulations, we have derived in continuum perturbation theory a formula for Wilson loops in three dimensions valid to fourth order in  $g$  for any compact semisimple Lie group. We present this derivation in Secs. II–VI. We use our Wilson-loop formula in Secs. VII and VIII to derive perturbative expressions valid to order  $g^4$  for the potential energy of a heavy quark-antiquark pair and for the Creutz ratio  $\chi(r,t)$ , which at large  $t$  approximates the  $q\bar{q}$  force.<sup>2</sup> In Sec. IX we modify these perturbative expressions to take account of periodic boundary conditions.

In Sec. X we present a critique of compact lattice gauge theory, describing four approximations that collectively cause compact lattice actions to be globally different from the Yang-Mills action. As a result of this difference, the distribution of the Yang-Mills action per plaquette in compact simulations is broader and shifted to larger values than that of the guiding compact action. The links of compact simulations thus are less correlated than those of simulations guided by the Yang-Mills action.

In Sec. XI we describe our noncompact method, which uses the Yang-Mills action, and explain why it is possible and preferable not to fix the gauge. In Sec. XII we discuss the Creutz ratios we measured for  $SU(2)$  in three dimensions both in noncompact simulations and in compact simulations, guided by Wilson's action as well as by Manton's.<sup>14</sup> Before renormalization, the Creutz ratios of the noncompact method are smaller than those of the perturbative formula; those obtained with Manton's action are larger than both; and those of Wilson's action are still larger. Although these differences can be partly absorbed by the renormalization of the two methods, the following trend remains: the forces predicted by the noncompact method fall off faster with distance than those of

the perturbative formula, while those of the compact method fall off slower. The noncompact simulations show no evidence for a linearly confining quark-antiquark potential. In Sec. XIII we discuss the renormalization of the two methods and explain why the unrenormalized Creutz ratios of the noncompact method are smaller than those of the perturbative formula.

A summary of the paper and a list of our conclusions appear in Sec. XIV.

## II. GROUP-THEORETIC PRELIMINARIES

The Wilson loop is related to the gauge-covariant group element  $G(x, y, \Gamma)$  that satisfies the time-ordered differential equation  $\mathcal{T}D_i(x)G(x, y, \Gamma) = 0$  along a path  $\Gamma$  from  $y$  to  $x$ . If the covariant derivative is taken as

$D_i(x) = \partial_i + ig A_i^a(x) T_a$ , then  $G$  is the exponential

$$G(x, y, \Gamma) = \mathcal{TP} \exp \left[ -ig \int_{\Gamma} A_i^a(x') T_a dx'_i \right]$$

in which the operators  $A_i^a(x)$  with Euclidean time dependence are time ordered and the generators  $T_a$  are path ordered. For a  $d$ -dimensional representation of the group, the Wilson loop  $W(r, t)$  is defined as the expected value of the trace of  $G(x, x, \Gamma)$  in the physical vacuum:

$$W(r, t) = \frac{1}{d} \langle \Omega | \text{Tr} [G(x, x, \Gamma)] | \Omega \rangle, \quad (2.1)$$

where the contour of integration  $\Gamma$  is an  $r$ -by- $t$  rectangle. The expansion of  $W(r, t)$  to fourth order in the coupling constant  $g$  is

$$\begin{aligned} W(r, t) = & 1 - \frac{g^2}{d} \text{Tr}(T_a T_b) \oint dx_i \int^x dy_j \langle \Omega | \mathcal{T} [A_i^a(x) A_j^b(y)] | \Omega \rangle \\ & + i \frac{g^3}{d} \text{Tr}(T_a T_b T_c) \oint dx_i \int^x dy_j \int^y dz_k \langle \Omega | \mathcal{T} [A_i^a(x) A_j^b(y) A_k^c(z)] | \Omega \rangle \\ & + \frac{g^4}{d} \text{Tr}(T_a T_b T_c T_d) \oint dx_i \int^x dy_j \int^y dz_k \int^z dw_l \langle \Omega | \mathcal{T} [A_i^a(x) A_j^b(y) A_k^c(z) A_l^d(w)] | \Omega \rangle. \end{aligned} \quad (2.2)$$

The first-order term is missing, even if some generators have nonzero traces, because the invariance of the action to the transformation  $A_i^a(x) \rightarrow -A_i^a(-x)$  implies that the mean values of the gauge fields vanish.

The first of the traces in this expansion is determined for semisimple groups by the orthogonality relation of the generators  $\text{Tr}(T_a T_b) = k \delta_{ab}$ , in which the normalization constant  $k$  is related to the quadratic Casimir invariant  $c = T_a^2$  and the number  $N$  of generators of the group by  $k = cd/N$ . The structure constants  $f_{abc}$  are

$$f_{abc} = \frac{-i}{k} \text{Tr}([T_a, T_b] T_c). \quad (2.3)$$

In what follows we shall only need the trace  $\text{Tr}(T_a T_b T_c)$  multiplied by  $f_{abc}$  and summed over  $a, b$ , and  $c$ . This sum is proportional to the quadratic Casimir invariant  $c_A$  of the adjoint representation:

$$\begin{aligned} \text{Tr}(T_a T_b T_c) f_{abc} &= \frac{1}{2} [\text{Tr}(T_a T_b T_c) - \text{Tr}(T_b T_a T_c)] f_{abc} \\ &= \frac{1}{2} \text{Tr}([T_a, T_b] T_c) f_{abc} \\ &= \frac{i}{2} \text{Tr}(T_d T_c) f_{abd} f_{abc} \\ &= \frac{ik}{2} f_{abc}^2 = \frac{ik}{2} N c_A = \frac{i}{2} c c_A d. \end{aligned} \quad (2.4)$$

To lowest order, the fourth term in the expansion (2.2) vanishes unless the group indices match in pairs, as in  $\text{Tr}(T_a^2 T_b^2)$  and  $\text{Tr}[(T_a T_b)^2]$ . The first of these traces is

$$\text{Tr}(T_a^2 T_b^2) = \text{Tr}(c^2) = c^2 d, \quad (2.5)$$

and the second differs from it by

$$\begin{aligned} \text{Tr}[(T_a T_b)^2] - \text{Tr}(T_a^2 T_b^2) &= -\text{Tr}(T_a [T_a, T_b] T_b) \\ &= i \text{Tr}(T_a T_b T_c) f_{abc} \\ &= -\frac{1}{2} c c_A d. \end{aligned} \quad (2.6)$$

The group  $\text{SU}(2)$  has  $N=3$  generators. Its defining representation has  $d=2$ , and we may use the Pauli matrices as the generators,  $T_a = \sigma_a/2$ , whence  $c = \frac{3}{4}$  and  $k = \frac{1}{2}$ . Its adjoint representation has  $d_A=3$ , and we may set  $(T_a)_{bc} = -i \epsilon_{abc}$ , so that  $c_A = k_A = 2$ . Thus for the defining representation of  $\text{SU}(2)$ , these trace formulas become  $\text{Tr}(T_a T_b) = \delta_{ab}/2$ ,  $\text{Tr}(T_a^2 T_b^2) = \frac{9}{8}$ , and  $\text{Tr}[(T_a T_b)^2] = -\frac{3}{8}$ . For the adjoint representation, they are  $\text{Tr}(T_a T_b) = 2\delta_{ab}$ ,  $\text{Tr}(T_a^2 T_b^2) = 12$ , and  $\text{Tr}[(T_a T_b)^2] = 6$ .

## III. THE WILSON LOOP TO ORDER $g^2$

The Euclidean propagator for the gauge field

$$\begin{aligned} D_{ij}^{ab}(x-y) &\equiv \langle \Omega | \mathcal{T} A_i^a(x) A_j^b(y) | \Omega \rangle \\ &= \int \frac{d^3 p}{(2\pi)^3} e^{ip \cdot (x-y)} \mathcal{D}_{ij}^{ab}(p) \end{aligned} \quad (3.1)$$

is given to lowest order in Feynman gauge by

$$\begin{aligned} D_{ij}^{(0)ab}(x-y) &= \int \frac{d^3 p}{(2\pi)^3} e^{ip \cdot (x-y)} \frac{\delta_{ij} \delta^{ab}}{p^2} \\ &= \frac{\delta_{ij} \delta^{ab}}{4\pi |x-y|}. \end{aligned} \quad (3.2)$$

Since  $\text{Tr}(T_a T_b) = k \delta_{ab}$ , the second-order contribution to the Wilson loop is

$$\begin{aligned}
W_2(r,t) &= -\frac{g^2}{d} k \delta_{ab} \oint dx_i \int^x dy_j D_{ij}^{(0)ab}(x-y) \\
&= -\frac{g^2 c}{8\pi} \oint dx_i \oint dy_i \frac{1}{|x-y|}, \quad (3.3)
\end{aligned}$$

where  $c = Nk/d$  is the quadratic Casimir of the representation. This doubly cyclic integral may be thought of as the sum of eight ordinary double integrals, in which  $x$  and  $y$  run over identical or parallel edges. These eight integrals are equal in pairs, so that only four are independent. Finally two of the four integrals may be obtained from the other two by interchanging  $r$  and  $t$ . We may therefore write  $W_2$  in the form

$$W_2(r,t) = U_2(r,t) + U_2(t,r) \quad (3.4)$$

where

$$\begin{aligned}
U_2(r,t) &= -\frac{g^2 c}{4\pi} \int_0^r dx_1 \int_0^r dy_1 \left[ \frac{1}{|x_1 - y_1|} \right. \\
&\quad \left. - \frac{1}{\sqrt{t^2 + (x_1 - y_1)^2}} \right] \\
&= \frac{g^2 c}{2\pi} [r \operatorname{arcsinh}(r/t) - r \ln(r/\epsilon) \\
&\quad - \sqrt{r^2 + t^2} + r + t], \quad (3.5)
\end{aligned}$$

in which  $\epsilon$  is an ultraviolet cutoff required by the singular color-electric string<sup>15</sup> generated by the group element  $G(x,y,\Gamma)$ . Since  $\epsilon$  enters  $W_2(r,t)$  in a term proportional to the perimeter of the loop,  $2r+2t$ , it does not contribute to the Creutz ratio, as we shall see in Sec. VIII.

#### IV. THE PROPAGATOR CORRECTION

There are three sources of the fourth-order contribution to the Wilson loop: the second-order correction to the propagator of the gauge field and the third and fourth terms in the expansion (2.2) of the Wilson loop. In this section we calculate the contribution to the Wilson loop from the propagator correction.

To one loop the propagator for the gauge field in the Feynman gauge is<sup>16,17</sup>

$$\mathcal{D}_{ij}^{ab}(p) = \delta^{ab} \left[ \frac{\delta_{ij} - \frac{p_i p_j}{p^2}}{p^2 - \frac{7g^2 c_A}{32} p} + \frac{p_i p_j}{p^2} \right], \quad (4.1)$$

which has a tachyonic pole (also known as a Landau ghost) at

$$p = p_t \equiv \frac{7g^2 c_A}{32}. \quad (4.2)$$

Near this pole the formula (4.1) for the propagator cannot be correct, and so we should use it only for  $p \gg p_t$ . At such large values of  $p$ , we might as well expand the denominator in powers of the coupling constant  $g$ , obtaining as the second-order correction to the propagator

$$\mathcal{D}_{ij}^{(2)ab}(p) = \delta^{ab} \left[ \delta_{ij} - \frac{p_i p_j}{p^2} \right] \frac{7g^2 c_A}{32p^3}. \quad (4.3)$$

By using this term to correct  $D_{ij}^{(0)ab}$  in Eq. (3.3), we may obtain its contribution to the Wilson loop as

$$\begin{aligned}
W_4^P(r,t) &= -\frac{g^2 \delta_{ab} k}{2d} \oint_{\Gamma} dx_i \oint_{\Gamma} dy_j \int \frac{d^3 p}{(2\pi)^3} e^{ip \cdot (x-y)} \\
&\quad \times \mathcal{D}_{ij}^{(2)ab}(p). \quad (4.4)
\end{aligned}$$

Since the correction (4.3) has the infrared singularity  $1/p^3$ , we regularize it by integrating over the space-time loop  $\Gamma$  before integrating over the momentum  $p$ . The double line integral around the  $r$ -by- $t$  rectangle  $\Gamma$  is

$$\begin{aligned}
K(p,r,t) &= \oint_{\Gamma} dx_i \oint_{\Gamma} dy_j \delta_{ij} e^{i(x-y) \cdot p} \\
&= 16 \left[ \frac{1}{p_1^2} + \frac{1}{p_3^2} \right] \sin^2 \left[ \frac{rp_1}{2} \right] \sin^2 \left[ \frac{tp_3}{2} \right]. \quad (4.5)
\end{aligned}$$

Because the  $p_i p_j$  term in the correction  $\mathcal{D}_{ij}^{(2)ab}(p)$  is a double partial derivative which does not contribute to loop integrals, the correction to the Wilson loop is the momentum integral of  $K(p,r,t)/p^3$ :

$$\begin{aligned}
W_4^P(r,t) &= -\frac{7g^4 N c_A k}{64d} \int \frac{d^3 p}{(2\pi)^3} \frac{K(p,r,t)}{p^3} \\
&= -\frac{7g^4 N c_A k}{64\pi d} r t. \quad (4.6)
\end{aligned}$$

For  $\sqrt{r^2 + t^2} \ll \pi/p_t$ , this integral is insensitive to momenta  $p$  of the order of  $p_t$  or smaller, where the one-loop propagator is inaccurate. Only for such small values of  $r$  and  $t$  is the formula (4.6) correct.

#### V. THE THIRD TERM IN THE WILSON-LOOP EXPANSION

To order  $g^4$ , the third term in the expansion (2.2) of the Wilson loop is the expected value in the bare vacuum of six gauge fields, of which three lie on the edges of the loop and three come from the cubic term in the Lagrangian:

$$W_4^{(3)}(r,t) = i \frac{g^4}{2d} \operatorname{Tr}(T_a T_b T_c) f_{deg} \oint dx_i \int^x dy_j \int^y dz_k \int d^3 w \langle 0 | \mathcal{T} [A_i^a(x) A_j^b(y) A_k^c(z) A_{[l,m]}^d(w) A_l^e(w) A_m^g(w)] | 0 \rangle. \quad (5.1)$$

Here  $A_{[l,m]}^d(w) \equiv A_{l,m}^d(w) - A_{m,l}^d(w)$  is the curl of the gauge field. By using the trace relation (2.4) and the formula  $D_{ij}^{(0)ab}(x) = \delta_{ij} \delta^{ab} / (4\pi|x|)$ , we may write  $W_4^{(3)}$  as

$$W_4^{(3)}(r,t) = \frac{g^4 c c_A}{2(4\pi)^3} \oint dx_i \int^x dy_j \int^y dz_k \int d^3w \frac{1}{|x-w||y-w||z-w|} \times \left[ \delta_{ij} \frac{\partial}{\partial w_k} \ln \frac{|x-w|}{|y-w|} + \delta_{jk} \frac{\partial}{\partial w_i} \ln \frac{|y-w|}{|z-w|} + \delta_{ki} \frac{\partial}{\partial w_j} \ln \frac{|z-w|}{|x-w|} \right]. \quad (5.2)$$

When  $i=j=k$ , the integrand vanishes, being proportional to the derivative of the logarithm of unity. In this section we reduce this six-dimensional integral to a three-dimensional one, which we have evaluated numerically.

We found it convenient to split this path-ordered integral into terms in which each of the loop coordinates  $x$ ,  $y$ , and  $z$  is integrated along an edge of the  $r$ -by- $t$  rectangle. For example, the term with  $x$  on the upper horizontal edge,  $y$  on the right vertical edge, and  $z$  on the lower horizontal edge, which we denote as  $R_x T_y r_z$ , is

$$R_x T_y r_z = \int_r^0 dx_1 \int_0^t dy_3 \int_0^r dz_1 \int d^3w \frac{1}{|x-w||y-w||z-w|} \frac{\partial}{\partial w_3} \ln \frac{|z-w|}{|x-w|}, \quad (5.3)$$

apart from the factor  $F = g^4 k N c_A / [2d(4\pi)^3]$ . The three edge integrals are easy because they decouple. For instance,

$$\int_0^t dy_3 \frac{1}{|y-w|} = \operatorname{arcsinh} \frac{w_3}{[(w_1-r)^2 + w_2^2]^{1/2}} - \operatorname{arcsinh} \frac{w_3-t}{[(w_1-r)^2 + w_2^2]^{1/2}}. \quad (5.4)$$

After using the symmetry of the integrand under the swap of  $w_3$  for  $t-w_3$ , we obtain

$$R_x T_y r_z = 2 \int d^3w \frac{w_3}{w_2^2 + w_3^2} \left[ \frac{w_1}{|w|} - \frac{w_1-r}{[(w_1-r)^2 + w_2^2 + w_3^2]^{1/2}} \right] \left[ \operatorname{arcsinh} \frac{w_1}{[w_2^2 + (w_3-t)^2]^{1/2}} - \operatorname{arcsinh} \frac{w_1-r}{[w_2^2 + (w_3-t)^2]^{1/2}} \right] \times \left[ \operatorname{arcsinh} \frac{w_3}{[(w_1-r)^2 + w_2^2]^{1/2}} - \operatorname{arcsinh} \frac{w_3-t}{[(w_1-r)^2 + w_2^2]^{1/2}} \right]. \quad (5.5)$$

The analogous term with  $x$  on the left vertical edge,  $y$  on the upper horizontal edge, and  $z$  on the lower horizontal edge, which we denote as  $t_x R_y r_z$ , is equal to  $R_x T_y r_z$ . There are two other terms like these but rotated by  $90^\circ$ ; they are also equal to each other and differ from  $R_x T_y r_z$  by the interchange of  $r$  with  $t$ .

The remaining terms in  $W_4^{(3)}(r,t)$  are ones with two loop coordinates on one edge and the third on a perpendicular edge. For example, the term with  $x$  on the right vertical edge and both  $y$  and  $z$  on the lower horizontal edge is

$$T_x r_y r_z = \int_0^t dx_3 \int_0^r dy_1 \int_0^{y_1} dz_1 \int d^3w \frac{1}{|x-w||y-w||z-w|} \frac{\partial}{\partial w_3} \ln \frac{|z-w|}{|y-w|}, \quad (5.6)$$

apart from the factor  $F$ . The  $x$  integral is given by (5.4). We may write the remaining integrand as  $G(y,z) - G(z,y)$  where  $G(y,z) = -|y-w|^{-1} \partial_3^w |z-w|^{-1}$  and thereby take advantage of the identity

$$\int_0^r dy_1 \int_0^{y_1} dz_1 [G(y,z) - G(z,y)] = 2 \int_0^r dy_1 \int_0^{y_1} dz_1 G(y,z) - \int_0^r dy_1 \int_0^r dz_1 G(y,z). \quad (5.7)$$

After evaluating these known integrals, we find

$$T_x r_y r_z = \int d^3w \frac{w_3}{w_2^2 + w_3^2} \left[ \operatorname{arcsinh} \frac{w_3}{[(w_1-r)^2 + w_2^2]^{1/2}} - \operatorname{arcsinh} \frac{w_3-t}{[(w_1-r)^2 + w_2^2]^{1/2}} \right] \times \left[ \left[ \operatorname{arcsinh} \frac{w_1}{(w_2^2 + w_3^2)^{1/2}} - \operatorname{arcsinh} \frac{w_1-r}{(w_2^2 + w_3^2)^{1/2}} \right] \left[ \frac{w_1}{|w|} + \frac{w_1-r}{[(w_1-r)^2 + w_2^2 + w_3^2]^{1/2}} \right] + \ln \frac{(w_1-r)^2 + w_2^2 + w_3^2}{|w|^2} \right]. \quad (5.8)$$

There are three other terms in which two loop coordinates lie on a single horizontal edge with the third on a vertical edge; all three are equal to  $T_x r_y r_z$ . There is also a quartet of terms with two loop coordinates on a single vertical edge and a third on a horizontal edge; they differ from the preceding quartet by an interchange of  $r$  with  $t$ .

We have now reduced  $W_4^{(3)}(r,t)$  to one complicated triple integral over space-time, essentially the sum of (5.5) and (5.8), which we have computed numerically.

## VI. THE FOURTH TERM IN THE WILSON-LOOP EXPANSION

In order to calculate to order  $g^4$  the quartic integral in the formula (2.2) for the Wilson loop, we found it convenient to write the path-ordered exponential in the definition (2.1) as the product of four path-ordered exponentials, one for each edge of the rectangle. We then expanded the path-ordered exponential for each edge in

powers of  $g$ , and kept all terms of order  $g^4$  in the product of the four exponentials. Each such term contains four gauge fields and is characterized by the edges along which the fields are integrated. The vacuum expected value of a given term consists of three pieces, each with two propagators and a distinct pairing of the fields in the propagators. For example, the term with all fields on the lower horizontal edge,

$$\frac{g^4}{d} \text{Tr}(T_a T_b T_c T_d) \int_0^r dx_1 \int_0^{x_1} dy_1 \int_0^{y_1} dz_1 \int_0^{z_1} dw_1 \times \langle \Omega | \mathcal{T} [A_1^a(x) A_1^b(y) A_1^c(z) A_1^d(w)] | \Omega \rangle, \quad (6.1)$$

contributes three terms, according to the order of the contractions:

$$\frac{g^4}{d} \text{Tr}(T_a^2 T_b^2) \int_0^r dx_1 \int_0^{x_1} dy_1 \int_0^{y_1} dz_1 \int_0^{z_1} dw_1 \times D_{11}(x-y) D_{11}(z-w), \quad (6.2)$$

$$\frac{g^4}{d} \text{Tr}[(T_a T_b)^2] \int_0^r dx_1 \int_0^{x_1} dy_1 \int_0^{y_1} dz_1 \int_0^{z_1} dw_1 \times D_{11}(x-z) D_{11}(y-w), \quad (6.3)$$

and

$$\frac{g^4}{d} \text{Tr}(T_a^2 T_b^2) \int_0^r dx_1 \int_0^{x_1} dy_1 \int_0^{y_1} dz_1 \int_0^{z_1} dw_1 \times D_{11}(x-w) D_{11}(y-z), \quad (6.4)$$

where  $D_{ij}(x) = \delta_{ij} / (4\pi|x|)$ . These traces, which are the only ones to occur in the order- $g^4$  terms, are evaluated in Eqs. (2.5) and (2.6).

In order to simplify the computations which follow, it is useful to recall<sup>8</sup> that for the group  $U(1)$  the Wilson loop (2.1) can be cast into the simple exact form  $W(r, t) = \exp[W_2(r, t)]$ , where  $W_2(r, t)$  is given by Eqs. (3.4) and (3.5) with  $c = 1$ . More generally for any Abelian group, the fourth-order contribution  $W_4^{(r)}(r, t)$  to the Wilson loop is always just  $\frac{1}{2}W_2(r, t)^2$  with the appropriate  $c$ . Thus if the coefficients of the three integrals (6.2)–(6.4) were all the same, then they would form  $\frac{1}{2}W_2(r, t)^2$  up to a numerical factor. So in each term like (6.1) we really only need to compute the integral analogous to (6.3) with the appropriate coefficient obtained from Eq. (2.6):

$$\frac{g^4}{d} \{ \text{Tr}[(T_a T_b)^2] - \text{Tr}(T_a^2 T_b^2) \} = -\frac{1}{2}g^4 cc_A. \quad (6.5)$$

In other words,  $W_4^{(r)}(r, t)$  differs from  $\frac{1}{2}W_2(r, t)^2$  only via terms in which the order of contractions is that of (6.3).

The multiple integral in Eq. (6.3) has all gauge fields on the lower horizontal edge  $r$  and has  $x$  paired with  $z$  and  $y$  with  $w$ ; we shall denote this integral multiplied by  $(4\pi)^2$  by the symbol  $r_x r_z r_y r_w$ :

$$r_x r_z r_y r_w \equiv \int_0^r dx_1 \int_0^{x_1} dy_1 \int_0^{y_1} dz_1 \int_0^{z_1} dw_1 \frac{1}{x_1 - z_1} \frac{1}{y_1 - w_1}. \quad (6.6)$$

To evaluate this integral, which is finite, we use the

indefinite integral of  $x(\ln x)^2$ , which is tabulated, and the definite integral

$$\int_0^1 du \ln u \ln(1-u) = 2 - \frac{\pi^2}{6}. \quad (6.7)$$

Then by interchanging the order of the  $y_1$  and  $z_1$  integrations in one of the terms, and using the symmetry of convolutions,

$$\int_0^y dz f(z)g(y-z) = \int_0^y dz f(y-z)g(z), \quad (6.8)$$

we find

$$r_x r_z r_y r_w = \pi^2 r^2 / 12. \quad (6.9)$$

The term analogous to (6.3) but with all fields integrated on the upper horizontal edge is in fact equal to (6.3) itself. There are also two terms like (6.3) but with all fields integrated on the right or left vertical edge; these are equal to (6.3) with  $r$  replaced by  $t$ . So we have now evaluated all terms in which all fields are integrated on a single edge.

Because the propagator is diagonal in the spin variable, any quartic term with three fields integrated on one edge must have the fourth field integrated on the opposite edge. The term with three fields integrated on the lower horizontal edge and one on the upper horizontal edge is

$$\frac{g^4}{d} \text{Tr}(T_a T_b T_c T_d) \int_r^0 dx_1 \int_0^r dy_1 \int_0^{y_1} dz_1 \int_0^{z_1} dw_1 \times \langle \Omega | \mathcal{T} [A_1^a(x) A_1^b(y) A_1^c(z) A_1^d(w)] | \Omega \rangle. \quad (6.10)$$

Letting  $R$  stand for the upper horizontal edge, we may write this term as

$$\frac{g^4}{(4\pi)^2 d} \{ \text{Tr}(T_a^2 T_b^2) R_x r_y r_z r_w + \text{Tr}[(T_a T_b)^2] R_x r_z r_y r_w + \text{Tr}(T_a^2 T_b^2) R_x r_w r_y r_z \}. \quad (6.11)$$

Once again we only need evaluate the second of these integrals:

$$R_x r_z r_y r_w \equiv \int_r^0 dx_1 \int_0^r dy_1 \int_0^{y_1} dz_1 \int_0^{z_1} dw_1 \frac{1}{[t^2 + (x_1 - z_1)^2]^{1/2}} \times \frac{1}{y_1 - w_1}. \quad (6.12)$$

We first integrate over  $x_1$  and  $w_1$  and then interchange the order of the  $y_1$  and  $z_1$  integrations, obtaining

$$R_x r_z r_y r_w = 2r^2 \mathcal{J}(r/t), \quad (6.13)$$

where

$$\mathcal{J}(v) \equiv \int_0^1 du [u \ln u + (1-u) \ln(1-u)] \text{arcsinh}(vu) \quad (6.14)$$

is an integral that we have evaluated numerically.

The term analogous to (6.12) but with three fields integrated on the upper horizontal edge is in fact equal to (6.12) itself. There are also two terms like (6.12) but with three fields integrated on the right or left vertical edge;

these are equal to (6.12) with  $r$  replaced by  $t$ . So we have now evaluated all terms in which three fields are integrated on a single edge.

We now consider the quartic term with two fields integrated on each of the horizontal edges,

$$\frac{g^4}{d} \text{Tr}(T_a T_b T_c T_d) \int_r^0 dx_1 \int_r^{x_1} dy_1 \int_0^r dz_1 \int_0^{z_1} dw_1 \times \langle \Omega | \mathcal{T}[A_1^a(x) A_1^b(y) A_1^c(z) A_1^d(w)] | \Omega \rangle, \quad (6.15)$$

which we may write as

$$\frac{g^4}{(4\pi)^2 d} \{ \text{Tr}(T_a^2 T_b^2) R_x R_y r_z r_w + \text{Tr}[(T_a T_b)^2] R_x r_z R_y r_w + \text{Tr}(T_a^2 T_b^2) R_x r_w R_y r_z \}. \quad (6.16)$$

Again we evaluate only the second of these integrals,

$$R_x r_z R_y r_w \equiv \int_r^0 dx_1 \int_r^{x_1} dy_1 \int_0^r dz_1 \int_0^{z_1} dw_1 \frac{1}{[t^2 + (x_1 - z_1)^2]^{1/2}} \times \frac{1}{[t^2 + (y_1 - w_1)^2]^{1/2}}, \quad (6.17)$$

in which the  $y_1$  and  $w_1$  integrals are easy. Then by integrating by parts and using the integral formulas,

$$\int dx [\text{arcsinh}(x/t)]^2 = x [\text{arcsinh}(x/t)]^2 - 2\sqrt{x^2 + t^2} \text{arcsinh}(x/t) + 2x \quad (6.18)$$

and

$$\int dx x [\text{arcsinh}(x/t)]^2 = (x^2/2 + t^2/4) [\text{arcsinh}(x/t)]^2 - (x/2) \sqrt{x^2 + t^2} \text{arcsinh}(x/t) + x^2/4, \quad (6.19)$$

we may reduce the remaining double integral to the form

$$T_x T_z R_y r_w \equiv \int_t^0 dx_3 \int_r^0 dy_1 \int_0^t dz_3 \int_0^r dw_1 \frac{1}{[r^2 + (x_3 - z_3)^2]^{1/2}} \frac{1}{[t^2 + (y_1 - w_1)^2]^{1/2}} = 4[r \text{arcsinh}(r/t) - \sqrt{r^2 + t^2} + t][t \text{arcsinh}(t/r) - \sqrt{r^2 + t^2} + r]. \quad (6.24)$$

This completes the evaluation of the order- $g^4$  terms in the expansion of  $W(r, t)$ . If we gather them all, then we may write the fourth-order term

$$W_4(r, t) = W_4^P(r, t) + W_4^{(3)}(r, t) + W_4^{(4)}(r, t) \quad (6.25)$$

in the form

$$W_4(r, t) = \frac{1}{2} W_2(r, t)^2 + U_4(r, t) + U_4(t, r) + W_4^{(3)}(r, t), \quad (6.26)$$

where  $W_4^{(3)}(r, t)$  is the triple integral of Sec. V which we have computed numerically and  $U_4(r, t)$  is

$$U_4(r, t) = -\frac{g^4 c c_A}{32\pi^2} \{ 2\pi r t + (r^2 + t^2/2) [\text{arcsinh}(r/t)]^2 + 2rt \text{arcsinh}(r/t) \text{arcsinh}(t/r) + (4r^2 + 2rt - 5r\sqrt{r^2 + t^2}) \text{arcsinh}(r/t) - 6r\sqrt{r^2 + t^2} + (\frac{9}{2} + \pi^2/6)r^2 + 2rt + 4r^2 \mathcal{J}(r/t) - 2r^2 \mathcal{J}(r/t) \}, \quad (6.27)$$

which is independent of the ultraviolet cutoff  $\epsilon$ .

$$R_x r_z R_y r_w = (r^2 + t^2/2) [\text{arcsinh}(r/t)]^2 + (2rt - r\sqrt{r^2 + t^2}) \text{arcsinh}(r/t) - 2t\sqrt{r^2 + t^2} - 3r^2/2 + 2t^2 - 2r^2 \mathcal{J}(r/t), \quad (6.20)$$

which involves a single integral

$$\mathcal{J}(v) \equiv \int_0^1 du [u \text{arcsinh}(vu) - \sqrt{u^2 + 1/v^2}] \times \text{arcsinh}[v(1-u)], \quad (6.21)$$

which we have evaluated numerically.

The term analogous to (6.17) but with the fields on the vertical edges is equal to (6.17) with  $r$  replaced by  $t$ .

We shall not evaluate the quartic term with two fields integrated on the lower horizontal edge and two on the right vertical edge  $T_x T_y r_z r_w$  because it does not contain a term of the required form (6.3), the propagator being diagonal in the spin variable. For the same reason, we do not consider the quartic term with two fields integrated on the lower horizontal edge and one on each vertical edge  $t_x T_y r_z r_w$ . Similarly we ignore another term with two fields integrated on the upper horizontal edge and one on each vertical edge  $t_x T_w R_y R_z$  and two analogous terms  $R_x r_w T_y T_z$  and  $t_x t_y R_z r_w$  which are related to them by the interchange of  $r$  with  $t$ .

Finally let us consider the quartic term with all four fields integrated on different edges of the loop,

$$\frac{g^4}{d} \text{Tr}(T_a T_b T_c T_d) \int_t^0 dx_3 \int_r^0 dy_1 \int_0^t dz_3 \int_0^r dw_1 \times \langle \Omega | \mathcal{T}[A_3^a(x) A_1^b(y) A_3^c(z) A_1^d(w)] | \Omega \rangle. \quad (6.22)$$

Because the propagator is diagonal in the spin variable, there is only one integral

$$\frac{g^4}{(4\pi)^2 d} \text{Tr}[(T_a T_b)^2] t_x T_z R_y r_w. \quad (6.23)$$

It has the same order of contractions as (6.3) and is given by

## VII. THE STATIC POTENTIAL

The Wilson loop  $W(r, t)$  may be written in the form<sup>15</sup>

$$W(r, t) = \exp[-tE(r) - D(r) - C(r, t)], \quad (7.1)$$

where  $E(r)$  is the energy of a static “quark-antiquark” pair,  $D(r)$  represents the overlap between the physical  $q\bar{q}$  state and the “string”  $q\bar{q}$  state

$$|q(r)\bar{q}(0)\rangle \sim q^\dagger(r)\mathcal{P} \exp\left[-ig \int_0^r A_i^a(x)T_a dx_i\right] \bar{q}^\dagger(0)|\Omega\rangle, \quad (7.2)$$

and  $C(r, t)$  represents the contribution of higher-energy states. The quantity  $D(r)$  diverges and the overlap  $e^{-D}$  vanishes because the electric flux of the string state (7.2) is infinitely intense along the string whereas the electric flux in the true  $q\bar{q}$  state is spread out and finite, except at the positions of the quarks. If, as we expect, the contribution  $C(r, t)$  of the higher-energy states has a vanishing time derivative in the limit  $t \rightarrow \infty$ , then we may express the energy of the static  $q\bar{q}$  pair as

$$E(r) = - \lim_{t \rightarrow \infty} \frac{\partial \ln W(r, t)}{\partial t}. \quad (7.3)$$

Apart from an infinite constant associated with the self-energies of the quarks, the energy  $E(r)$  is the  $q\bar{q}$  static potential  $V(r)$ , which we shall now compute to order  $g^4$ .

To fourth order in the coupling constant, the Wilson loop is  $W = 1 + W_2 + W_4$ , where  $W_2$  and  $W_4$  are given by Eqs. (3.4) and (6.26). We may therefore expand  $\ln W(r, t)$  as

$$\begin{aligned} \ln W(r, t) &= W_2(r, t) + W_4(r, t) - \frac{1}{2}W_2(r, t)^2 \\ &= U_2(r, t) + U_2(t, r) + U_4(r, t) + U_4(t, r) \\ &\quad + W_4^{(3)}(r, t). \end{aligned} \quad (7.4)$$

The cutoff  $\epsilon$  enters  $\ln W(r, t)$  only through  $U_2$  in the form of a term proportional to the perimeter of the loop. Hence the Creutz ratio  $\chi(r, t)$  is independent of the cutoff, as we shall see. However the cutoff does contribute self-energy terms to  $E(r)$ .

By studying the time derivative of  $\ln W$  analytically, we have found that the only contributions to  $E(r)$  in the limit  $t \rightarrow \infty$  are those due to the second-order term  $U_2(t, r)$  and the fourth-order propagator correction  $W_4^{(3)}(r, t)$ . Thus after subtracting the infinite self-energy terms, we may express the  $q\bar{q}$  static potential to order  $g^4$  as

$$V(r) = \frac{g^2 c}{2\pi} \ln(r/2a) + \frac{g^4 cc_A}{8\pi} r, \quad (7.5)$$

apart from an additive constant. The linear confinement exhibited by this formula for the static potential may be spurious, however, because the tachyonic pole (4.2) in the one- and two-loop perturbative propagators<sup>16,17</sup> invalidates our formula for  $W_4^P(r, t)$  when  $r$  or  $t$  exceeds  $\pi/p_t = 32\pi/(7g^2 c_A)$ .

In checking numerically the formula (7.5) for the potential  $V(r)$ , we have found that the convergence as  $t \rightarrow \infty$  of the time derivative of  $-\ln W(r, t)$  to its limiting form (7.5) is surprisingly slow. For example, for  $g = 2$  the value of  $-\partial \ln W_4^{(4)}(3a, t)/\partial t$  is 0.7220 at  $t = 3a$ , 0.1807 at  $t = 30a$ , 0.0287 at  $t = 300a$ , 0.0037 at  $t = 3000a$ , and  $-0.0001$  at  $t = 30000a$ . These values suggest that to get accurate potentials from Monte Carlo data on Wilson loops requires very large lattices in three space-time dimensions. However, the convergence of the time derivative of  $\ln W(r, t)$  should be much faster in four dimensions.

## VIII. THE CREUTZ RATIO

One may avoid the infinite self-energies in the energy  $E(r)$  of static quarks separated by a distance  $r$ , by computing the magnitude  $f(r)$  of the force between them,

$$f(r) = - \lim_{t \rightarrow \infty} \frac{\partial^2 \ln W(r, t)}{\partial r \partial t}. \quad (8.1)$$

A form of this derivative suitable for lattice calculations has been introduced by Creutz:<sup>2</sup>

$$\chi(r, t) = - \ln \left[ \frac{W(r, t)W(r-a, t-a)}{W(r, t-a)W(r-a, t)} \right]. \quad (8.2)$$

In terms of this Creutz ratio  $\chi(r, t)$ , the force  $f(r)$  is the limit

$$f(r) = \lim_{\substack{t \rightarrow \infty \\ a \rightarrow 0}} \frac{\chi(r, t)}{a^2}. \quad (8.3)$$

In this section, we shall use our perturbative formula for  $\ln W(r, t)$  to numerically evaluate  $\chi(r, t)$  for small  $r$  and  $t$ .

In lattice gauge theory it is convenient to describe distances in terms of the lattice spacing  $a$  and to use a dimensionless inverse coupling  $\beta$  that is defined, for a  $d$ -dimensional representation of a group with generators normalized according to  $\text{Tr}(T_a T_b) = k \delta_{ab}$  in  $D$ -dimensional space-time, as  $\beta \equiv a^{D-d} / kg^2$ . By using Eq. (7.4), we may write  $\ln W(r, t)$  to second order in  $1/\beta$  as

$$\ln W(r, t) = U(r/a, t/a) + U(t/a, r/a) + W_4^{(3)}(r, t), \quad (8.4)$$

where with  $\rho = r/a$  and  $\tau = t/a$  the function  $U(\rho, \tau)$  is

$$\begin{aligned} U(\rho, \tau) &= \frac{cd}{2\pi k \beta} [\rho \text{arcsinh}(\rho/\tau) - \rho \ln(\rho) - \rho \ln(a/\epsilon) - \sqrt{\rho^2 + \tau^2} + \rho + \tau] \\ &\quad - \frac{cc_A d^2}{32\pi^2 k^2 \beta^2} \{ 2\pi\rho\tau + (\rho^2 + \tau^2/2) [\text{arcsinh}(\rho/\tau)]^2 + 2\rho\tau \text{arcsinh}(\rho/\tau) \text{arcsinh}(\tau/\rho) \\ &\quad + (4\rho^2 + 2\rho\tau - 5\rho\sqrt{\rho^2 + \tau^2}) \text{arcsinh}(\rho/\tau) - 6\rho\sqrt{\rho^2 + \tau^2} \\ &\quad + (\frac{9}{2} + \pi^2/6)\rho^2 + 2\rho\tau + 4\rho^2 \mathcal{J}(\rho/\tau) - 2\rho^2 \mathcal{F}(\rho/\tau) \}. \end{aligned} \quad (8.5)$$

We may now obtain a formula for the Creutz ratio  $\chi(r, t)$  by substituting the expressions (8.4) and (8.5) into its definition (8.2). Since  $\ln W(r, t)$  depends upon the ultraviolet cutoff  $\epsilon$  only through a term proportional to  $r + t$ , the Creutz ratio is finite and independent of the cutoff.

We have numerically evaluated our formula for  $\chi(r, t)$  for the case of small square loops. The results may be expressed as

$$\chi(r, t) = \frac{cd}{2\pi k\beta} f(r/a, t/a) + \frac{cc_A d^2}{32\pi^2 k^2 \beta^2} s(r/a, t/a), \quad (8.6)$$

where the coefficients are  $f(2, 2) = 0.98973$ ,  $f(3, 3) = 0.57535$ ,  $f(4, 4) = 0.40754$ ,  $f(5, 5) = 0.31590$ ,  $f(6, 6) = 0.25802$  and  $s(2, 2) = 8.791$ ,  $s(3, 3) = 8.771$ ,  $s(4, 4) = 8.766$ ,  $s(5, 5) = 8.764$ ,  $s(6, 6) = 8.764$ .

Our perturbative formula for  $\chi(r, t)$  is only reliable when  $g$ ,  $r$ , and  $t$  are sufficiently small that the fourth-order term in  $\chi(r, t)$  is smaller than the second-order term and that  $W_4^P(r, t)$  is insensitive to the tachyonic pole (4.2) in the gauge propagator. The second of these conditions is the more restrictive, requiring

$$[(r/a)^2 + (t/a)^2]^{1/2} \ll \frac{32\pi c}{7Nc_A} \beta. \quad (8.7)$$

For  $SU(2)_3$ , the range of validity is  $\beta \gg 1$  and  $\sqrt{(r/a)^2 + (t/a)^2}$  much less than  $1.8\beta$ .

Because of the rotational symmetry of the Euclidean action, the Creutz ratio, like the Wilson loop, is symmetric:  $\chi(r, t) = \chi(t, r)$ .

Other finite ratios, like that of Creutz's, have been considered<sup>18</sup> and may be evaluated by steps analogous to (8.2)–(8.5).

### IX. CORRECTION FOR PERIODIC BOUNDARY CONDITIONS

Monte Carlo simulations must be carried out on finite lattices, and so require boundary conditions on the surface of the lattice. These boundary conditions, which we have taken to be simply periodic, have an effect on the Creutz ratio  $\chi(r, t)$ . To estimate this effect, we shall now calculate these ratios to order  $g^2$  in a version of the continuum theory on which periodic boundary conditions have been imposed.

If the fields of the continuum theory are required to be periodic with period  $La$ , then the Euclidean gauge-field propagator

$$D_{ij}^{ab}(x-y) \equiv \langle \Omega | T A_i^a(x) A_j^b(y) | \Omega \rangle$$

in the Feynman gauge is

$$D_{ij}^{ab}(x-y) = \frac{\delta^{ab} \delta_{ij}}{(La)^3} \sum_p \frac{e^{ip \cdot (x-y)}}{p^2 + \mu^2}, \quad (9.1)$$

where the vector  $p$  is related to a vector  $\mathbf{n}$  of integers  $n_1$ ,  $n_2$ , and  $n_3$  by  $p = 2\pi \mathbf{n} / (La)$ . We have regularized the zero mode  $p = 0$  by adding to the denominator  $p^2$  a fictitious mass term  $\mu^2$ , which we shall set equal to zero after

summing over  $n_2$ .

One may obtain the order- $g^2$  contribution  $W_2(r, t)$  to the Wilson loop of the periodic continuum theory by integrating this propagator over the loop as in Eq. (3.3). At  $r = ka$  and  $t = ma$ , the resulting  $W_2(r, t)$  is

$$W_2(ka, ma) = -\frac{c dL}{2k\beta\pi^4} \sum_n \frac{1}{n^2 + \epsilon^2} \left[ \frac{1}{n_1^2} + \frac{1}{n_3^2} \right] \times \sin^2 \left[ \frac{\pi n_1 k}{L} \right] \sin^2 \left[ \frac{\pi n_3 m}{L} \right], \quad (9.2)$$

where  $\epsilon = La\mu / (2\pi)$ . By using the identity

$$\sum_{n=-\infty}^{\infty} \frac{1}{n^2 + \alpha^2} = \frac{\pi}{\alpha} \coth(\pi\alpha), \quad (9.3)$$

which may be established by a contour integration, one may write  $W_2(ka, ma)$  in the form

$$W_2(ka, ma) = -\frac{c dL}{2k\beta\pi^3} \sum_{\substack{n_1=-\infty \\ n_3=-\infty \\ (n_1, n_3) \neq (0,0)}}^{\infty} \frac{(n_1^2 + n_3^2)^{1/2}}{\tanh[\pi(n_1^2 + n_3^2)^{1/2}]} \frac{1}{n_1^2} \frac{1}{n_3^2} \times \sin^2 \left[ \frac{\pi n_1 k}{L} \right] \sin^2 \left[ \frac{\pi n_3 m}{L} \right], \quad (9.4)$$

after setting the fictitious mass  $\mu$  equal to zero. The term omitted from the sum cancels in Creutz ratios.

We have substituted this expression for  $W_2$ , which is  $\ln W$  to order  $g^2$ , into the definition (8.2) of the ratio  $\chi(r, t)$  and have done the sums numerically. The effect of this correction for periodic boundary conditions is to reduce the ratio by a factor that grows with the length of the loop and shrinks with the size of the lattice. For a  $16^3$  lattice, the decrease in  $\chi(na, na)$  to order  $g^2$  is 0.47% for  $n = 2$ , 2.30% for  $n = 3$ , 6.58% for  $n = 4$ , 14.61% for  $n = 5$ , and 28.01% for  $n = 6$ .

Periodic boundary conditions reduce Creutz ratios because they in effect create copies of the lattice, so that a quark sends its color-electric flux not only to its antiquark partner but also to the images of that antiquark. Thus the  $q\bar{q}$  force and the Creutz ratios which measure it are smaller.

We have estimated the effect of periodic boundary conditions upon each of the fourth-order terms  $W_4^P$ ,  $W_4^{(3)}$ , and  $W_4^{(4)}$  by using the relative correction of  $W_2$  as many times as the term contains propagators. Since this estimate is based on little more than a guess, it represents another theoretical uncertainty, one that grows with the size of the loop and shrinks with  $\beta$ . On a  $16^3$  lattice at  $\beta = 60$ , this theoretical uncertainty runs from about 0.04% for  $\chi(2, 2)$  to about 8% for  $\chi(6, 6)$ . The corresponding uncertainties at  $\beta = 10$  are about 0.2% for  $\chi(2, 2)$ , 6% for  $\chi(4, 4)$ , and 15% for  $\chi(5, 5)$ .



With these corrections for periodicity on a  $16^3$  lattice, our perturbative formula (8.6) for the Creutz ratio becomes

$$\chi_P(r,t) = \frac{cd}{2\pi k\beta} f_P(r/a, t/a) + \frac{cc_A d^2}{32\pi^2 k^2 \beta^2} s_P(r/a, t/a), \quad (9.5)$$

where the coefficients for small square loops are  $f_P(2,2)=0.98506$ ,  $f_P(3,3)=0.56210$ ,  $f_P(4,4)=0.38072$ ,  $f_P(5,5)=0.26975$ ,  $f_P(6,6)=0.18575$  and  $s_P(2,2)=8.631$ ,  $s_P(3,3)=8.016$ ,  $s_P(4,4)=6.748$ ,  $s_P(5,5)=4.812$ ,  $s_P(6,6)=2.605$ . Some values of  $\chi_P(r,r)$  for SU(2) are listed in Table II below.

### X. CRITIQUE OF COMPACT LATTICE GAUGE THEORY

In compact lattice gauge theory, the basic variables are the link variables  $l_i(x) \equiv \exp[-iga A_i^b(x) T_b]$  which are

elements of the compact gauge group and here are labeled by the vertex  $x$  from which they emanate and the direction  $i$  in which they point. The Wilson action is made from the sum over all plaquettes of the path-ordered product  $U_p$  of the link variables around the plaquette

$$S_W = \beta \sum_p \left[ 1 - \frac{1}{d} \text{Re Tr}(U_p) \right]. \quad (10.1)$$

For a plaquette in the  $i$ - $j$  plane, the unitary matrix  $U_p \equiv U_{ij} = \exp(ia^2 g F_{ij})$  is the exponential of a Hermitian field-strength matrix  $F_{ij} \equiv F_{ij}^b T_b$  which is related to the gauge fields  $A_i \equiv A_i^b T_b$  of the links of the plaquette by the infinite Hausdorff series for the group product  $l_{-j} l_{-i} l_j l_i$ :

$$F_{ij} = \frac{A_i(x+ae_j) - A_i(x)}{a} - \frac{A_j(x+ae_i) - A_j(x)}{a} - \frac{ig}{2} [A_i(x), A_j(x+ae_i)] - \frac{ig}{2} [A_i(x+ae_j), A_j(x)] - \frac{ig}{2} [A_i(x+ae_j) + A_j(x), A_i(x) + A_j(x+ae_i)] + \dots, \quad (10.2)$$

where  $e_i$  is a unit vector in the  $i$ th direction. When the fields of adjacent parallel links differ by a quantity of first order in the lattice spacing, the field strength to that order is

$$F_{ij} = \frac{A_i(x+ae_j) - A_i(x)}{a} - \frac{A_j(x+ae_i) - A_j(x)}{a} - ig [\bar{A}_i(x), \bar{A}_j(x)], \quad (10.3)$$

where  $\bar{A}_i(x) = \frac{1}{2} [A_i(x+ae_j) + A_i(x)]$  with a similar formula for  $\bar{A}_j(x)$ . An expansion of the unitary matrix  $U_{ij}$  gives for the Wilson action the series

$$S_W = \frac{a^D}{4} \sum_{\text{cubes}} (F_{ij}^a)^2 + \dots \quad (10.4)$$

in which the first term is formally the Yang-Mills action.

In addition to Wilson's structure of links and plaquettes, compact lattice gauge theory uses four approximations that are potential sources of error.

(1) The compactification of the domain of integration to the group manifold.

(2) The use of the Hausdorff formula (10.2) instead of the Yang-Mills formula (10.3) as the relation between the field strength  $F_{ij}$  and the field  $A_i$ .

(3) The use of compact lattice actions that are functions of the plaquette matrices. Such actions sometimes slough off part of the field strength (10.2).

(4) The inclusion in the Wilson action (10.4) of the infinite series of terms that comes from the expansion of  $U_{ij}$  beyond the quadratic term.

The first three approximations are intrinsic to Wilson's method. They are the price of exact lattice gauge invariance. Manton's action avoids the fourth approximation.

These four approximations add to the perturbative action extra terms that contribute to the largeness of the ratio<sup>19</sup> of the continuum and lattice QCD scale parameters:  $\Lambda_{\alpha=1}^{\text{MOM}} / \Lambda^{\text{lattice}} = 83.5$ .

The first approximation is legitimate only when the fields are small and the group elements close to the identity. In general the topology and curvature of the group manifold require an invariant measure  $dg$  which adds the term  $-\ln|dg/dA|$  per link to the Wilson action. For SU(2) the effective Wilson action is

$$S_W^{\text{eff}} = S_W - 2 \sum_{\text{links}} \ln \left[ \frac{\sin(ag|\mathbf{A}_i|/2)}{ag|\mathbf{A}_i|/2} \right] \quad (10.5)$$

which restricts the fields to the ball  $ag|\mathbf{A}_i| \leq 2\pi$ . The first approximation correlates the fields: even at  $\beta=0$  the mean value  $ag \langle |\mathbf{A}_i| \rangle$  of the dimensionless field is  $\pi$ .

We may appreciate the effect of the second approximation by multiplying both sides of the Hausdorff formula (10.2) by  $a^2 g$  and so expressing the dimensionless field strength  $a^2 g F_{ij}$  as a power series in the fields  $ag A_i$ . Because of lattice gauge invariance, the mean values  $ag \langle |\mathbf{A}_i| \rangle$  in our compact simulations do attain the analytic value of  $\pi$  for all  $\beta$ . Even after the links have been gauge transformed as close as possible to the identity, the mean values of the fields remain substantial—e.g., at  $\beta=2$  Wilsonian simulations give  $ag \langle |\mathbf{A}_i| \rangle = 1.12$ . So when the fields do not commute, the cubic and higher-order terms in the series (10.2) are comparable to the linear and quadratic ones, and the series is more a burlesque of the Yang-Mills formula (10.3) than an approximation to it. Since the relative importance of the derivatives is thereby diminished, the second approximation decorrelates the fields.

The third approximation also decorrelates the fields. Compact lattice actions, such as Wilson's

$$S_W = \frac{\beta}{d} \sum_p \sum_{k=1}^d (1 - \cos \theta_k) \quad (10.6)$$

or Manton's, are functions of the unimodular eigenvalues  $e^{i\theta_k}$  of the plaquette matrices  $U_{ij}$  and thus are periodic in the phases  $\theta_k$ . So although these phases are proportional to the diagonalized dimensionless field strengths,  $\theta_k \delta_{kl} = a^2 g (F_{ij}^{\text{diag}})_{kl} \pmod{2\pi}$ , they in effect lie within the interval  $[-\pi, \pi]$ . For example, in the Abelian theory  $U(1)$ , if the link variables  $l_i, l_j, l_{-i}$ , and  $l_{-j}$  are all  $e^{i\phi}$ , then for  $|\phi| < \pi/4$  the phase  $\theta$  is  $4\phi$  and both the Wilson action and the Yang-Mills action of that plaquette are approximately  $\beta(4\phi)^2/2$ . But as  $\phi$  grows beyond  $\pi/4$ ,  $\theta$  jumps from  $\pi$  to  $-\pi$  and then starts shrinking. For  $\phi = \pi/2$  and  $\pi$ ,  $\theta = 0$  and the Wilson action vanishes, but the Yang-Mills action is  $\beta(2\pi)^2/2$  and  $\beta(4\pi)^2/2$ , respectively.

Because of their quasiperiodicity, compact lattice actions possess multiple minima which represent false vacua not present in the continuum theory. For  $SU(2)$  Wilson's action per plaquette is  $S_W = \beta[1 - \cos(f/2)]$  where  $f = a^2 g \text{Tr}(F_{ij}^{\text{diag}} \sigma_3)$  is the dimensionless field strength. The false vacua are at  $f = 4\pi$  and  $8\pi$  as shown in Fig. 1. At equilibrium the plaquettes populate all the vacua. So in simulations guided by these actions, the fields are insufficiently damped and excessively decorrelated. This excessive decorrelation of the fields makes a major contribution to the string tension, as has been

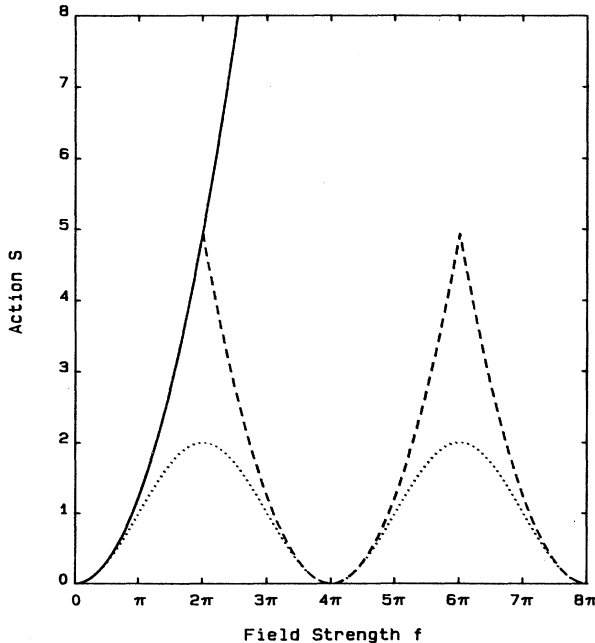


FIG. 1. For  $SU(2)$  at  $\beta=1$  the Yang-Mills action is plotted as a function of the field strength  $f$  of a plaquette as a solid line, Wilson's action as a dotted line, and Manton's as a dashed line. The false vacua at  $f = 4\pi$  and  $8\pi$  are clearly visible.

shown in simulations by Mack and Pietarinen<sup>20</sup> and by Grady.<sup>21</sup> In their simulations of  $SU(2)$  in four dimensions, they modified the Wilson action in gauge-invariant ways by erecting, in effect, infinite potential barriers between the true vacuum and the false vacua. The first of these barriers lies between  $f = \pi$  and  $f = 3\pi$  in Fig. 1. Mack and Pietarinen found a sharp drop in the string tension; Grady found no string tension at all.

In the unmodified Wilson method, the false vacua at weak coupling are separated from the true vacuum by high potential barriers; so it takes a great many sweeps for the plaquettes to sneak around these barriers and populate the false vacua. The phenomenon of critical slowing down, observed in compact simulations at weak coupling, may be partly due to the many sweeps required to achieve an equilibrium population of plaquettes about the false vacua.

Because the group manifold is not spherical, except in special cases such as  $SU(2)$ , the gap between a compact action and the Yang-Mills action in general depends upon the direction of the field strength in the Lie algebra. Compact lattice gauge theory is thus intrinsically astigmatic. The case of  $SU(3)$  is displayed in Fig. 2.

The fourth approximation also decorrelates the fields. The Wilson action (10.6) being essentially a sum of cosines allows much larger excursions of the fields than does the Yang-Mills action which is quadratic in the field strengths. The third and fourth approximations thus not only overly decorrelate the fields, they also exacerbate the

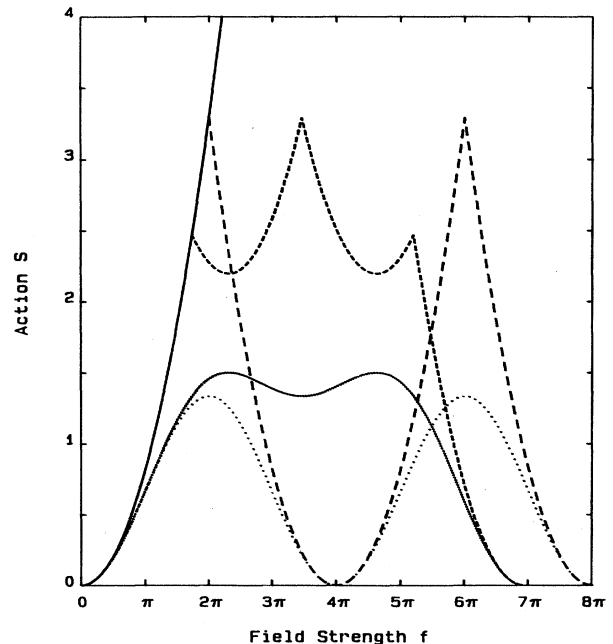


FIG. 2. The Yang-Mills action of  $SU(3)$  at  $\beta=1$  is graphed as a solid line. The dashed lines display Manton's action—the longer dashes are for field strengths along the  $\lambda_3$  direction and the shorter ones are for those along the  $\lambda_8$  direction. The dotted lines display Wilson's action—the densely dotted line for  $\lambda_8$  and the other one for  $\lambda_3$ . The false vacua and the astigmatism are obvious.

errors of the first two approximations, which are valid only when the fields are small.

The fourth approximation, like the third, also causes the Wilson action to depend upon the direction of the field strength in the Lie algebra, thereby adding to the astigmatism of the third approximation. For Wilson's action lacks those symmetries that accrue to the Yang-Mills action by virtue of its being a sum of squares of field strengths. Some of these symmetries constitute the Euclidean group of space-time rotations. Others are invariances to transformations that rotate the field strengths by transforming the fields nonlinearly. These latter symmetries may not be very pretty; but an action should assign the same weight to fields whose field strengths are related by a global rotation, which Wilson's action fails to do in general.

We may illustrate this lack of rotational symmetry by considering the unitary groups and SU(3) in particular. For SU( $n$ ) one may diagonalize both the plaquette group element  $U_{ij} = \exp(ia^2 g F_{ij})$  and the field strength  $F_{ij}$  by an SU( $n$ ) transformation and so express the eigenphases  $\theta_i$  of  $U_{ij}$  as

$$\theta_k \delta_{kl} = a^2 g (F_{ij}^{\text{diag}})_{kl} \pmod{2\pi}. \quad (10.7)$$

The diagonalized field-strength matrix  $F_{ij}^{\text{diag}}$  is a linear combination of the generators  $H_m$  of the Cartan subalgebra of SU( $n$ ):  $a^2 g F_{ij}^{\text{diag}} = \sum_{m=1}^{n-1} f^m H_m$ . By using explicit formulas<sup>22</sup> for the  $H_m$ 's, one may express the eigenphases  $\theta_k$ , which lie between  $-\pi$  and  $\pi$ , as linear combinations of the dimensionless field strengths  $f^m$ :

$$\theta_k = (1 - \delta_{kn}) \left[ \sum_{m=i}^{n-1} \frac{f^m}{\sqrt{2m(m+1)}} \right] - (1 - \delta_{k1}) \frac{(i-1)f^{i-1}}{\sqrt{2i(i-1)}} \pmod{2\pi}. \quad (10.8)$$

One may use this expression to write the Wilson action (10.6) in terms of the field strengths  $f^m$ .

For SU(3) the generators  $H_m$  are just half the Gell-Mann matrices  $\lambda_3$  and  $\lambda_8$ :

$$H_1 = T_3 = \frac{1}{2}\lambda_3 = \frac{1}{2}\text{diag}(1, -1, 0)$$

and

$$H_2 = T_8 = \frac{1}{2}\lambda_8 = (1/2\sqrt{3})\text{diag}(1, 1, -2).$$

Modulo  $2\pi$ , the angles  $\theta_k$  are

$$\theta_1 = \frac{f^1}{2} + \frac{f^2}{2\sqrt{3}}, \quad \theta_2 = -\frac{f^1}{2} + \frac{f^2}{2\sqrt{3}}, \quad \text{and} \quad \theta_3 = -\frac{f^2}{\sqrt{3}}. \quad (10.9)$$

So the Wilson action assumes the astigmatic form

$$S_W = \beta \sum_p \left\{ 1 - \frac{1}{3} \left[ \cos \left[ \frac{f^1}{2} + \frac{f^2}{2\sqrt{3}} \right] + \cos \left[ \frac{f^1}{2} - \frac{f^2}{2\sqrt{3}} \right] + \cos \left[ \frac{f^2}{\sqrt{3}} \right] \right] \right\}, \quad (10.10)$$

which is generally higher when  $(f^1, f^2) = (0, f)$  than

when  $(f^1, f^2) = (f, 0)$ , as shown in Fig. 2. However, for small field strengths,  $|f| \leq 1$ , the difference is less than 3 parts in 80 000.

The errors due to the fourth approximation can be avoided by the use of the Manton action  $S_M$  which is just the desirable part of the Wilson action:

$$S_M = \frac{\beta}{2d} \sum_p \text{Tr}(\ln U_{ij}^\dagger \ln U_{ij}) = \frac{\beta}{2d} \sum_p \sum_{k=1}^d \theta_k^2. \quad (10.11)$$

When the dimensionless field strengths  $f^m$  are so small that the periodicity of the eigenphases  $\theta_i$  can be ignored, Manton's action is formally equal to the Yang-Mills action

$$S_{YM} = \frac{a^D}{2k} \sum_p \text{Tr}(F_{ij}^2) = \frac{\beta}{4d} \sum_p \sum_{m=1}^r (f^m)^2, \quad (10.12)$$

where  $r$  is the rank of the gauge group. For SU(3) Manton's action per plaquette is  $S_M = (\beta/6)(\theta_1^2 + \theta_2^2 + \theta_3^2)$  with the  $\theta$ 's given by Eq. (10.9). Simulations guided by Manton's action have higher field correlations than those guided by Wilson's, an effect also seen in SU(2)<sub>4</sub> by Lang, Rebbi, Salomonson, and Skagerstam.<sup>18</sup>

In Fig. 1 Manton's action and Wilson's are graphed for SU(2). The maxima of  $S_M$  at  $f = 2\pi$  and  $4\pi$  are more than twice as high as those of  $S_W$ . For SU(3) the astigmatism of the two actions (10.10) and (10.11) and their false vacua are evident in Fig. 2 which displays these actions as functions of the dimensionless field strengths  $f^m$ . The limits on the  $f^m$ 's are four times those imposed on the dimensionless fields  $ag|A_i|$  by compactification, to wit:  $f^1 \leq 8\pi$  and  $f^2 \leq 4\sqrt{3}\pi$ . Both compact actions are periodic in the field strength  $f^1$  with period  $4\pi$  and in  $f^2$  with period  $4\sqrt{3}\pi$ . Clearly neither Wilson's action nor Manton's globally mimics the Yang-Mills action.

To determine the extent to which the four approximations of compact lattice gauge theory introduce errors that are statistically significant, we have measured the Yang-Mills action in compact simulations of SU(2)<sub>3</sub> both guided by Wilson's action and by Manton's on a  $16^3$  lattice. For each link variable  $l_i(x)$ , we took the gauge field to be  $A_i(x) = i \ln[l_i(x)]/(ga)$ . As a lattice analogue of the Yang-Mills action per plaquette, we used  $S_{YM} = a^3 \text{Tr}(F_{ij}^2)$ , where the field-strength matrix  $F_{ij}$  is given by Eq. (10.3), not the Hausdorff formula (10.2).

In the simulations guided by Wilson's action, the mean value  $\langle S_{YM} \rangle$  of the Yang-Mills action per plaquette was about  $7.5\beta$  for  $0.5 \leq \beta \leq 10$ , while that of the Wilson action  $\langle S_W \rangle$  never exceeded 1.14. In the simulations guided by Manton's action, the corresponding mean values were very similar. Thus in our compact simulations, the mean value of the Yang-Mills action was bigger than that of the guiding compact action by about an order of magnitude at strong coupling and by nearly 2 orders of magnitude at weak coupling. Figure 3 shows the mean Yang-Mills action  $\langle S_{YM} \rangle$  per plaquette for SU(2)<sub>3</sub> on successive sweeps from cold starts in compact simulations at  $\beta = 10$ .

However, if one is only interested in measuring quantities that are invariant under lattice gauge transformations, then much of this action gap may be considered to

TABLE I. In compact simulations, the mean value  $\langle S_{YM} \rangle$  and standard deviation of  $\sigma_{YM}$  of the Yang-Mills action per plaquette and of the guiding action, whether Wilson's  $S_W$  or Manton's  $S_M$ , for various  $\beta$ .

$\beta$	0.5	1.0	2.0	3.0	4.0	6.0	8.0	10.0
$\langle S_{YM} \rangle$	0.89	1.47	1.83	1.61	1.35	1.19	1.13	1.11
$\sigma_{YM}$	0.73	1.35	1.90	1.68	1.21	1.01	0.95	0.91
$\langle S_W \rangle$	0.44	0.76	1.09	1.14	1.09	1.05	1.02	1.03
$\sigma_W$	0.25	0.47	0.79	0.88	0.85	0.86	0.82	0.82
$\langle S_{YM} \rangle$	0.79	1.16	1.25	1.17	1.12	1.07	1.07	1.04
$\sigma_{YM}$	0.68	1.10	1.22	1.05	0.94	0.88	0.87	0.85
$\langle S_M \rangle$	0.52	0.80	0.97	1.00	1.00	1.00	1.01	1.01
$\sigma_M$	0.38	0.80	0.79	0.82	0.82	0.81	0.82	0.82

be a lattice gauge artifact. For one may take the view that the correspondence  $A_i(x) = i \ln[l_i(x)] / (ga)$  between the links of a compact simulation and the fields of a non-compact simulation should be made only after one smoothes the links by a lattice gauge transformation that brings them as close to the identity as possible. We simulated such a smoothing lattice gauge transformation by making several hundred sweeps through the lattice with an algorithm that maximized the sum of the traces  $\text{Tr}(l_i)$  of the six links of each vertex by a gauge transformation.

After such gauge smoothing, the mean values and standard deviations of the Yang-Mills action  $\langle S_{YM} \rangle$  and of the guiding compact action, either Wilson's  $\langle S_W \rangle$  or

Manton's  $\langle S_M \rangle$ , were as shown in Table I. The mean value  $\langle S_{YM} \rangle$  of the Yang-Mills action in gauge-smoothed simulations guided by Wilson's action rose from 0.89 at  $\beta=0.5$  to 1.83 at  $\beta=2$  and then declined to 1.11 at  $\beta=10$ . The corresponding mean value  $\langle S_W \rangle$  of Wilson's action in these simulations was 0.44 at  $\beta=0.5$ , 1.09 at  $\beta=2$ , and 1.03 at  $\beta=10$ . At  $\beta=2$ , the gap between the Yang-Mills action and the guiding Wilson action,  $\langle S_{YM} \rangle - \langle S_W \rangle = 0.74$ , was nearly as big as the guiding action itself,  $\langle S_W \rangle = 1.09$ ; and the standard deviation,  $\sigma_{YM} = 1.90$ , of the Yang-Mills action was more than twice as big as that of Wilson's action,  $\sigma_W = 0.79$ . After gauge smoothing, the mean value  $\langle S_{YM} \rangle$  of the Yang-Mills action in simulations guided by Manton's action rose from 0.79 at  $\beta=0.5$  to 1.25 at  $\beta=2$  and then declined to 1.04 at  $\beta=10$ . The corresponding mean value  $\langle S_M \rangle$  of Manton's action was 0.52 at  $\beta=0.5$ , 0.97 at  $\beta=2$ , and 1.01 at  $\beta=10$ . At  $\beta=2$ , the action gap between the Yang-Mills action and the guiding Manton action,  $\langle S_{YM} \rangle - \langle S_M \rangle = 0.28$ , was about 29% of the guiding action  $\langle S_M \rangle = 0.97$ ; and the standard deviation,  $\sigma_{YM} = 1.22$ , of the Yang-Mills action was about 54% bigger than that of Manton,  $\sigma_M = 0.79$ .

As these data indicate, the gauge smoothing reduced the action gaps dramatically but to levels that seem to us too high, particularly for the simulations guided by Wilson's action. The distributions of the Yang-Mills action are also broader than those of the guiding compact actions. Figure 4 is a histogram of the actions  $S_W$  and  $S_{YM}$  of the gauge-smoothed plaquettes of three independent sweeps at  $\beta=2$ .

To estimate the statistical significance of the color astigmatism in compact simulations of  $SU(3)$ , we have measured the ratio  $\langle \text{Tr}[F_{ij}^{\text{diag}} \lambda_3]^2 \rangle / \langle \text{Tr}[F_{ij}^{\text{diag}} \lambda_8]^2 \rangle$  of the squares of the two eigenvalues of the diagonalized field strength of Eq. (10.3) on a lattice consisting of a single plaquette. At  $\beta=6$  Wilson's method gave for this ratio 1.9, the noncompact method 1.0. Had we first gauge smoothed the links, however, the compact astigmatism ratio would probably have been much closer to unity.

In compact lattice gauge theory, the measurement of quantities that are not invariant to lattice gauge transformations seems to require gauge smoothing of the links.

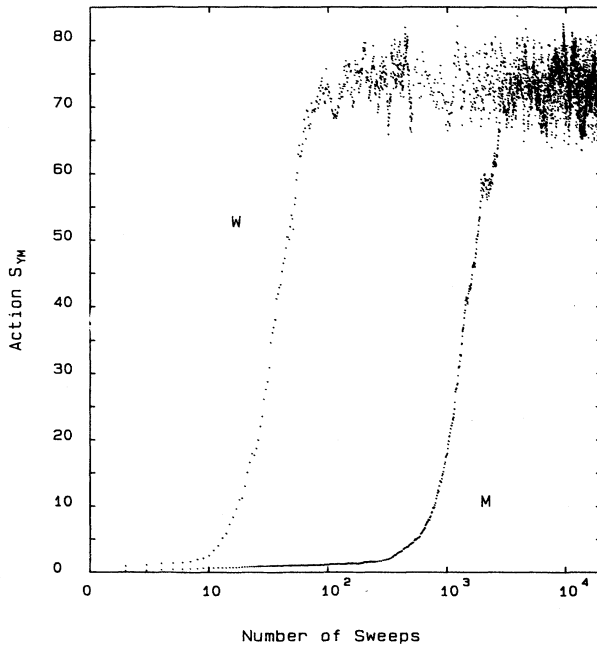


FIG. 3. The mean Yang-Mills action  $\langle S_{YM} \rangle$  per plaquette on the first 20 000 sweeps of two compact simulations of  $SU(2)_3$  from cold starts on an  $8^3$  lattice at  $\beta=10$ . In the simulation guided by Wilson's action, the mean action rises steeply after about ten sweeps; in the other guided by Manton's action, the steep rise occurs after about 500 sweeps.

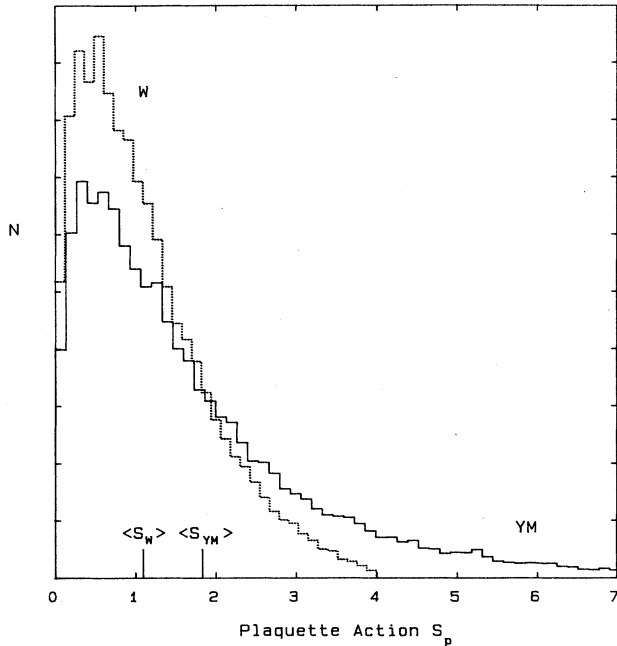


FIG. 4. For  $SU(2)_3$ , a histogram of the Yang-Mills action  $S_{YM}$  and the Wilson action  $S_W$  on the plaquettes of a  $16^3$  lattice on three independent sweeps of a simulation at  $\beta=2$  guided by Wilson's action after gauge smoothing. The mean values are  $\langle S_{YM} \rangle = 1.83$  and  $\langle S_W \rangle = 1.09$ , and the standard deviations are  $\sigma_{YM} = 1.90$  and  $\sigma_W = 0.79$ . The tail of the  $S_{YM}$  distribution extends to 28.7.

## XI. OUR NONCOMPACT METHOD

Our noncompact method<sup>9-13</sup> for approximating ratios of Euclidean path integrals avoids the four Wilsonian approximations. We tile space-time with simplices, linearly interpolate the fields throughout each simplex from their values at the vertices, and so define the fields continuously throughout space-time. We use the action and domain of integration of the exact continuum theory, unaltered apart from the granularity of the simplicial lattice. Thus we give exactly the right weight  $e^{-S}$  to each linearly interpolated field configuration. In the limit in which the lattice spacing goes to zero and the lattice size to infinity, the space of linearly interpolated fields over which we integrate becomes dense in the space of continuous fields. In this limit the method defines, at least formally, the Euclidean functional integral of the continuum theory. For it is with such a limiting process and the Trotter product formula that one derives the path-integral version of the continuum theory from its temporal-gauge Hilbert-space formulation.

In applications of this method to problems in three dimensions, we limit space-time to a periodic cubic lattice, each primitive cube of which is tiled with six (tetrahedral) simplices as shown in Fig. 5. Each space-time point  $x$  lying in a simplex with vertices  $v_n$  is of the form  $x = \sum_n \rho_n v_n$  in which the four non-negative weights  $\rho_n$  depend linearly upon  $x$ , are unique, and sum to unity. We use this formula to linearly interpolate the field

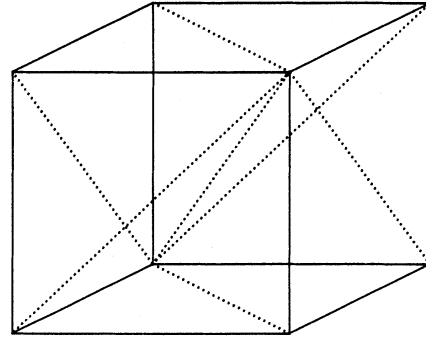


FIG. 5. A cube of the lattice divided into six tetrahedral simplices.

$A_i^a(x)$  to  $x$  from its values  $A(i, a, v_n)$  at the vertices  $v_n$  as  $A_i^a(x) = \sum_n \rho_n A(i, a, v_n)$ . Since the interpolated fields are defined throughout space-time, we use the Euclidean action of the continuum theory. For a gauge theory without matter fields, we take  $S(A) = \int d^3x \frac{1}{4} F_{ij}^a(x)^2$ , where  $F_{ij}^a(x)$  is defined in terms of the interpolated field  $A_i^a(x)$  as in the continuum theory without gauge fixing. Thus we approximate the mean value in the vacuum of a Euclidean-time-ordered operator  $Q(A)$  by a normalized multiple integral over the  $A(i, a, v)$ 's:

$$\langle \Omega | \mathcal{T}Q(A) | \Omega \rangle \approx \frac{\int e^{-S(A)} Q(A) \prod_{i,a,v} dA(i,a,v)}{\int e^{-S(A)} \prod_{i,a,v} dA(i,a,v)} \quad (11.1)$$

This formula suffers from only two approximations: (1) in the multiple integrals the sum is only over linearly interpolated fields, rather than over all fields, and (2) space-time is limited to a finite cubic lattice with periodic boundary conditions.

To be gauge invariant, a formulation of a gauge theory must satisfy two requirements. The first is the fundamental requirement, called Gauss's law, which is a constraint arising from the absence of the time derivatives of the fields  $A_0^a$  in the action of the theory. The second is the technical requirement that the mean values of gauge-invariant operators be independent of the gauge in which one quantizes the theory and does perturbative calculations. After explaining why the preceding ratio (11.1) of multiple integrals is well defined in our method without gauge fixing, we shall describe how in our method we implement Gauss's law by integrating over all gauges and how we satisfy the two requirements of gauge invariance.

It is usual in continuum perturbation theory to fix the gauge so as to invert the kinetic term in the action. This reason for fixing the gauge does not apply to our method since we are approximating ratios of path integrals non-perturbatively without inverting the kinetic term. We now show why the ratio (11.1) of integrals is well defined without gauge fixing and why it is, in fact, better not to fix the gauge.

Were we somehow analytically performing the full continuum path integration over all gauges and then taking the ratio in Eq. (11.1), we would be summing over redun-

dant fields and encountering in the numerator and denominator divergences which would cancel. But in our Monte Carlo approach, we merely evaluate the function  $Q(A)$  at successive field configurations  $A_n$ ,

$$\langle Q(A) \rangle = \frac{1}{N} \sum_{n=1}^N Q(A_n), \quad (11.2)$$

and so the extra gauge copies introduce no divergences. There is only a small inefficiency due to the use of  $D$  fields where  $D-1$  would suffice with gauge fixing.

We may illustrate these last ideas by means of a toy example. Suppose we wished to compute the mean value of  $q(a)$  in a theory in which the action  $S(a,b)=S(a)$  was independent of  $b$ :

$$\langle q(a) \rangle = \frac{\int_{-\infty}^{\infty} da \int_{-\infty}^{\infty} db e^{-S(a)} q(a)}{\int_{-\infty}^{\infty} da \int_{-\infty}^{\infty} db e^{-S(a)}}. \quad (11.3)$$

Both the numerator and the denominator have the divergent factor  $\int_{-\infty}^{\infty} db$  which cancels. A Monte Carlo evaluation avoids these divergences by expressing the mean value  $\langle q(a) \rangle$  as a sum

$$\langle q(a) \rangle = \frac{1}{N} \sum_{n=1}^N q(a_n) \quad (11.4)$$

over  $N$  pairs  $(a_n, b_n)$ . This procedure is somewhat inefficient in that the work done in choosing the  $N$  values of the irrelevant gauge degree of freedom  $b$  is wasted.

To see why it is actually better not to fix the gauge in our method, even if one could avoid the Gribov ambiguity,<sup>23</sup> let us consider the continuum theory formulated in the temporal gauge. In principle this formulation requires the use of an operator  $\Pi_G$  that projects onto the subspace of states that satisfy Gauss's law. This operator is generally omitted because the operator  $\Pi_V \equiv \lim_{t \rightarrow \infty} e^{-iH}$  that projects onto the physical vacuum also projects onto this subspace. If we enforce Gauss's law by redundantly inserting the operator  $\Pi_G$  at every time slice, then in the continuum limit we transform ratios of temporal-gauge path integrals into ratios of path integrals without gauge fixing. In lattice simulations, the length  $t=La$  of the time axis is quite limited by practical considerations, and so the projection operator  $\Pi_V$  onto the physical vacuum is not fully realized and does not guarantee Gauss's law. Thus in lattice simulations it is necessary either to insert the projection operator  $\Pi_G$  explicitly or to integrate over all gauges. Since it is difficult to implement the operator  $\Pi_G$ , we have chosen to integrate over all gauges in our method.

In the evaluation of the mean values of gauge-invariant operators, one may wonder how integrating over all gauges can be any different from fixing the gauge. For finite cubic lattices with periodic boundary conditions, the difference is due to the fact that it is not possible to transform an arbitrary field that is periodic on the lattice into an arbitrary gauge while maintaining its periodicity. For instance, in an Abelian theory, if a periodic field  $A_i(x,t)$  with period  $L$  is to be transformable into a periodic field in the temporal gauge, then it must satisfy the condition

$$0 = \int_0^L \partial_i A_0(x,t) dt \quad (11.5)$$

for  $i=1,2$ . So if one fixes the gauge, one loses some fields.

Because our method uses the exact gauge-invariant classical action  $S$ , it assigns the correct weight  $e^{-S}$  to each linearly interpolated field. As noted above, the method integrates only over fields that satisfy periodic boundary conditions on the surface of a cubic lattice and that vary linearly through the tetrahedra with which we have tiled the lattice. These linearly interpolated fields seem to us to be distributed throughout the space of all continuous fields in a very uniform manner. Moreover since the space of piecewise linear functions is dense in the space of continuous functions, it follows that as the periodic lattice becomes infinite and as the lattice spacing shrinks to zero, the space of linearly interpolated fields becomes dense in the space of all continuous fields. In this continuum limit, we suppose that the method becomes exact, at least if the bare parameters of the Lagrangian are adjusted according to a suitable renormalization prescription. If the method does become exact in this limit, then it will respect Gauss's law and all the physical symmetries of the continuum theory.

Short of this limit, the domain of functional integration is incomplete and the accuracy of the approximation afforded by the method for any particular ratio (11.1) of Euclidean path integrals will depend on the lattice spacing, the size of the periodic lattice, and the operator whose mean value is being evaluated. In an actual simulation, Gauss's law and the physical symmetries of the theory, such as Poincaré invariance, will be respected only up to the accuracy of the approximation.

Gauge symmetry, being a mathematical rather than a physical symmetry, is not a symmetry of the Hilbert space of the theory. In temporal-gauge quantization, for example, the operators representing time-dependent gauge transformations do not leave the Hilbert space invariant. And unlike the case of a physical symmetry, there is no way to decide whether a formulation of a theory satisfies the technical requirement of gauge invariance without comparing it with other formulations to see whether the mean values of gauge-invariant operators are independent of the gauge in which the theory is quantized. Our method, which is based upon temporal-gauge quantization with an explicit implementation of Gauss's law, uses a gauge-invariant action without any gauge fixing, at least in the continuum limit. Since we integrate over all gauges, we feel that the technical requirement of gauge invariance is less crucial for our method than for perturbation theory. Moreover for our method, this requirement refers to whether, if we fixed the gauge by various gauge conditions, introducing gauge-fixing terms and their Faddeev-Popov compensations, and if we measured various gauge-invariant operators in the different gauges, then we would find equal mean values. Since, as we have mentioned above, gauge fixing is not always possible on finite periodic lattices, these gauge-fixing procedures are of limited validity for our method, except in the continuum limit. So we expect that in most cases the mean values that we might compute without gauge fixing would be more accurate than those that one might compute in any particular gauge.

In the continuum limit, the space of linearly interpolated fields becomes dense in the gauge-invariant space of all continuous fields. Short of this limit, the space of linearly interpolated fields is invariant under global gauge transformations, but not under local ones because under a local continuum gauge transformation our interpolated fields lose their linear dependence on space-time. Moreover, because the group of continuum gauge transformations has continuously infinitely many parameters, no space of fields invariant under it can be stored in a finite digital computer. The image  $A'$  of a linearly interpolated field  $A$  under a local gauge transformation  $g(x)$  varies nonlinearly with  $x$ , but has a unique best linear approximation  $A'_L$ . The respective actions are nearly equal,  $S(A) = S(A') \approx S(A'_L)$ , when the gauge transformation varies little on the scale of one lattice spacing.<sup>12,24</sup> In an earlier work,<sup>12</sup> we compared the Wilson loops of our method with and without temporal gauge fixing. We found that the agreement between the two sets of loops improved as the lattice spacing shrank and as the size of the lattice increased. We expect that in the continuum limit the noncompact method completely respects the technical requirement of gauge invariance. It is worth noting that both the action and the gauge invariance of compact lattice gauge theory are also approximations to the action and gauge invariance of the continuum theory that become exact only in this same continuum limit.

Actually there are two practical advantages to the fact that the space of linearly interpolated fields is not exactly gauge invariant. The first is that the method thereby has something of the efficiency of a gauge-fixed method in that no computation of redundant gauge copies is performed. The second is that the fields are not obliged to drift out along the directions of gauge transformations to unmanageably great magnitudes.

The compact method has an exact lattice gauge symmetry that is different from the gauge invariance of the continuum theory. It achieves this exact lattice symmetry by compromising the fields and action of the continuum theory, as we have seen in the preceding section, whereas the noncompact method respects the fields and action of the continuum theory. It is not clear which side of this trade-off is more accurate for non-Abelian theories. The noncompact method is clearly better for Abelian theories. For  $U(1)$  the noncompact method is accurate at all coupling strengths,<sup>10</sup> whereas the compact method is accurate only at weak coupling.

Compact simulations of Abelian gauge theories exhibit deconfining phase transitions at weak coupling. It has recently been suggested that this is also the case for non-Abelian theories. Thus Grady<sup>21,25</sup> has found that the  $SU(2)$  theory in four dimensions is consistent with a correlation-length exponent  $\nu \approx \frac{2}{3}$  and a critical point  $\beta_c \approx 2.47$ . For  $SU(3)$  he found  $\nu \approx 1$  and  $\beta_c \approx 6.69$ . Patrascioiu, Seiler, Linke, and Stamatescu<sup>26</sup> argue that all zero-temperature lattice gauge theories in three or more dimensions must undergo a phase transition that is the limit of the finite-temperature deconfining transition. For  $SU(2)$  on a small lattice, they found  $\beta_c \approx 2.3$ . If these phase transitions are real and lead to a deconfined phase, then it is possible that the compact method in that phase

agrees with the noncompact one.

If the compact and noncompact methods both have an unconfined gauge theory as their continuum limit, then we may have to adopt Gribov's picture<sup>4</sup> of quark confinement. In his view pure gauge theories do not confine quarks. Rather quark confinement occurs because at moderate distances the gauge-field forces are strong enough, by asymptotic freedom, to pair-produce very light quarks. A similar view, involving a condensate of light quark-antiquark pairs, has been advanced by Grady.<sup>21</sup>

If the compact method does not have deconfining phase transitions, then the two methods disagree, unless on very large lattices the noncompact method should display confinement. More work is required to tell whether one, both, or neither method is right.

Other physicists<sup>5-8</sup> have eschewed Wilson's four approximations by using noncompact methods with simple, discrete actions. Because they did not interpolate the fields or use the continuum action, they had to fix the gauge to prevent the fields from diffusing to infinity. In our noncompact simulations, the fields diffuse to infinity with the number of sweeps only for *Abelian* gauge groups. In a run of 10 000 sweeps for  $SU(2)_3$  at  $\beta = 2.5$  on a  $4^3$  lattice, the mean value  $\langle |ga A_i^b| \rangle$  was 0.7022 on the first 150 sweeps and 0.6999 on the last 1700. In our method we do not need to fix the gauge to prevent the fields from diffusing to infinity.

The multiple integrals in Eq. (11.1) are of too high a dimension ( $> 10^4$ ) to be approximated by classical methods of quadrature. We use a Monte Carlo algorithm that was initiated by Fermi, developed by Metropolis, and improved by Creutz.<sup>27</sup> This heat-bath algorithm is feasible for our action  $S(A)$  for  $SU(2)_3$ , which on a  $16^3$  lattice is a quartic polynomial in 36 864  $A(i, a, v)$ 's, because each  $A$  occurs only quadratically in  $S(A)$ , due to the antisymmetry of  $F_{ij}^a(x)$ , and is coupled to only 135 other  $A$ 's in 24 simplices. No matter what the gauge group, Creutz's heat-bath algorithm requires only the first and second derivatives of the noncompact action with respect to each  $A(i, a, v)$ . We used<sup>11</sup> MACSYMA to calculate these derivatives and to write them in FORTRAN. The resulting source code is about 67 kbytes.

In the noncompact method, since the fields are interpolated throughout space-time, one may approximate the path ordering in the definition (2.1) of the Wilson loop to arbitrary precision. We divided each lattice spacing along the loop into  $n(\beta)$  subintervals and used an ordered product of  $n(\beta)$  exponentials, one for each subinterval. To determine  $n(\beta)$ , we assumed that the Wilson loops fell off with loop size according to an area law from the easily measured smaller loops and required that  $n(\beta)$  be high enough to ensure that the error in approximating the loop  $W(6a, 6a)$  on each sweep be less than 1% of average value of that loop as extrapolated by the area law. We found that it was sufficient to take  $n(\beta) \sim 150/\beta$  for  $\beta \geq 2$ . Thus we used 75 subintervals for  $\beta = 2$ , 50 for  $\beta = 3$ , 35 for  $\beta = 4$ , 25 for  $\beta = 6$ , 20 for  $\beta = 8$ , but, for good measure, 50 for  $\beta = 10$  and 60.

However at stronger coupling the larger Wilson loops are small, and we face three problems in trying to mea-



sure them accurately. First, we need very small errors and therefore exceedingly long runs. Second, the number of subintervals must be large, which slows the code. Third, we must use double precision when the value of the Wilson loop is less than about  $10^{-5}$ . At  $\beta=1$ , for example, the extrapolated value of  $W(5a, 5a)$  is of the order of  $10^{-4}$ . To measure this loop to within 10% would require about 200 000 sweeps with 150 subintervals. We therefore ran with 100 subintervals at  $\beta=1$  which is more than sufficient to measure  $W(4a, 4a)$ . For similar reasons we ran in single precision using 100 subintervals also at  $\beta=0.5$  and  $0.25$ , which is more than sufficient to measure  $W(3a, 3a)$  and  $W(2a, 2a)$ , respectively.

The noncompact method as described here is about an order of magnitude slower than the compact method. This slowness limited the number of thermalizing and measurement sweeps that we could run, and may limit the ultimate usefulness of this version of the method, at least until faster machines become available. For our work in four dimensions, we have relaxed somewhat the interpolation of the fields and have much increased the speed of the code.

## XII. MONTE CARLO MEASUREMENTS OF CREUTZ RATIOS

To measure Wilson loops and their Creutz ratios  $\chi(r, t)$  by means of the noncompact method, we used a  $16^3$  periodic lattice and began from cold starts in which all fields were initialized to zero. We allowed 900 sweeps for thermalization at  $\beta=0.25$ , 400 at  $\beta=0.5$ , 1750 at  $\beta=1$ , 400 at  $\beta=2$  and  $3$ , 500 at  $\beta=4$  and  $6$ , 600 at  $\beta=8$ , 2100 at  $\beta=10$ , and 1600 at  $\beta=60$ . We measured Wilson loops on every sweep, except for  $\beta=10$  and  $60$  where we skipped every other sweep. We made each measurement of the Wilson loop  $W(r, t)$  by averaging the 24 576 different  $r$ -by- $t$  loops that occur in a  $16^3$  lattice, including periodic translations and rotations by  $\pi/2$ . We made 1300 measurements at  $\beta=0.25$ , 1550 at  $\beta=0.5$ , 1100 at  $\beta=1$ , 800 at  $\beta=2$ , 700 at  $\beta=3$ , 600 at  $\beta=4$  and  $6$ , 500 at  $\beta=8$ , and 400 at  $\beta=10$  and  $60$ .

We have also measured Creutz ratios by doing compact simulations, both guided by Wilson's action and by Manton's. We ran these simulations on a  $16^3$  lattice, using codes based on those of Otto *et al.* For the case of Wilson's action, we used a heat-bath algorithm and allowed 1500 sweeps for thermalization at  $\beta=0.5$ , 2200 at  $\beta=1$ , 2100 at  $\beta=2$ , 8050 at  $\beta=3$ , 3000 at  $\beta=4$ , 4000 at  $\beta=6$ , 3000 at  $\beta=8$  and  $10$ , and 10 000 at  $\beta=60$ . After these thermalizing sweeps, we measured Wilson loops on every third sweep. We made 700 measurements at  $\beta=0.5$  and  $1$ , 1400 at  $\beta=2$ , 750 at  $\beta=3$ , 300 at  $\beta=4$ , 200 at  $\beta=6$ ,  $8$ , and  $10$ , and 800 at  $\beta=60$ .

For the case of Manton's action we used a simple Monte Carlo algorithm and allowed 1500 sweeps for thermalization at  $\beta=0.5$ , 1850 at  $\beta=1$ , 1900 at  $\beta=2$ , 3200 at  $\beta=3$ , 3000 at  $\beta=4$  and  $6$ , 8000 at  $\beta=8$ , 7250 at  $\beta=10$ , and 10 000 at  $\beta=60$ . After these thermalizing sweeps, we measured Wilson loops on every fifth sweep for  $\beta \leq 8$  and every tenth sweep otherwise. We made 600 measurements at  $\beta=0.5$ , 1400 at  $\beta=1$ , 500 at  $\beta=2$ , 400 at  $\beta=3$ , 300 at  $\beta=4$ , 200 at  $\beta=6$ ,  $8$ , and  $10$ , and 500 at

$\beta=60$ .

Some of our values for the Creutz ratios  $\chi(r, r)$  are listed in Table II. For the measured ratios,  $\beta$  is unrenormalized; for the perturbative ones it is renormalized. Our errors are indicated within parentheses; for instance,  $1.72(25)$  means  $1.72 \pm 0.25$ . In estimating these errors, we assumed that the loops of successive measurements were independent. These errors are purely statistical and do not include any systematic errors due to the insufficient thermalization or measurement. By examining the variation of the Wilson loops as the number of sweeps increased, we judged that we had allowed a sufficient number of thermalizing sweeps to compensate for any critical slowing down, even at  $\beta=60$ . Because the noncompact method is slower, we allowed fewer thermalizing sweeps in our noncompact simulations than in our compact ones. But noncompact simulations are free of false vacua and so probably require fewer thermalizing sweeps. Moreover at weak coupling the loops we measured are all much smaller than the correlation length and so we expect that critical slowing down is not important in our measurements.

Our perturbative formula for  $\chi_P(r, t)$  is plausible only when the fourth-order term is smaller than the second-order term. Thus by formula (9.5), the limits of validity for  $\chi_P(r, r)$  are  $\beta$  greater than 1.4, 2.4, 3.2, and 3.8 for  $r/a=2, 3, 4$ , and  $5$ , respectively. Only values of  $\chi_P(r, r)$  within these bounds are displayed in Table II. However, because of the tachyonic pole in the one-loop gauge propagator (4.1), our perturbative formula is reliable only for  $r$  and  $t$  that satisfy the inequality (8.7). For such  $r$  and  $t$ , the theoretical uncertainty in our estimate of the order- $g^4$  correction for periodicity on a  $16^3$  lattice is small.

At equal values of  $\beta$ , the noncompact  $\chi_{NC}$ 's are smaller than those of the perturbative formula, for reasons that we shall explain in the following section on renormalization. The  $\chi$ 's of the compact simulations are larger than the perturbative  $\chi_P$ 's, probably because the links of the compact simulations are overly decorrelated. The Wilson  $\chi_W$ 's are larger than the Manton  $\chi_M$ 's probably because Manton's action avoids the fourth approximation of Wilson's method. Our values for  $\chi_{NC}$  differ from those reported by Yotsuyanagi.<sup>7</sup> Our results for the case of Wilson's action agree with prior measurements.<sup>28</sup> The differences  $\chi_W - \chi_{NC}$  and  $\chi_M - \chi_{NC}$  are commensurate with the action gaps  $\langle S_{YM} \rangle - \langle S_W \rangle$  and  $\langle S_{YM} \rangle - \langle S_M \rangle$ . Published results<sup>5,6,18,26</sup> and our preliminary data suggest that the hierarchy  $\chi_{NC} < \chi_W < \chi_M$  also holds for  $SU(2)_4$ .

By using Eq. (8.3) with  $t=6a$  instead of infinity, we crudely measured the  $q\bar{q}$  force of the noncompact method at  $\beta=10$  in units of  $a^{-2}$  to be  $f(1.5a)=0.0281(10)$ ,  $f(2.5a)=0.0139(16)$ ,  $f(3.5a)=0.0081(22)$ ,  $f(4.5a)=0.0053(29)$ , and  $f(5.5a)=0.0040(45)$ , which resembles a  $r^{-1.5}$  force law. At  $\beta=60$ , again with  $t=6a$ , we found  $f(1.5a)=0.0053(2)$ ,  $f(2.5a)=0.0030(3)$ ,  $f(3.5a)=0.0020(4)$ ,  $f(4.5a)=0.0015(5)$ , and  $f(5.5a)=0.0011(8)$ , which resembles a  $1/r$  force law. To really determine the force law it would be necessary to measure Wilson loops with  $t \gg 6$  with high statistics.

Our noncompact simulations, like Nešić's<sup>8</sup> but unlike



TABLE II. Creutz ratios from the noncompact method, from the order- $g^4$  perturbative formula corrected for periodicity, and from the compact method guided by Manton's action and by Wilson's with errors in parentheses. For the Monte Carlo data, the values of  $\beta$  are unrenormalized.

$\beta$	$\frac{r}{a}, \frac{t}{a}$	Noncompact	$O(g^4)$ Pert.	Manton	Wilson
0.25	2,2	1.72(25)			
0.5	2,2	0.651(7)		1.41(10)	2.79(165)
	3,3	0.36(28)			
1.0	2,2	0.319(2)		1.047(9)	1.462(52)
	3,3	0.136(9)			
	4,4	0.067(55)			
2.0	2,2	0.169 4(8)	0.399 1	0.512(3)	0.766(3)
	3,3	0.071 3(29)		0.491(27)	0.608(110)
	4,4	0.028 1(72)			
3.0	2,2	0.117 3(6)	0.229 7	0.280(1)	0.408(2)
	3,3	0.052 9(18)	0.157 1	0.244(6)	0.365(11)
	4,4	0.022 3(42)		0.195(31)	0.203(122)
	5,5	0.008 9(79)			
4.0	2,2	0.090 0(4)	0.158 6	0.184(1)	0.237(1)
	3,3	0.041 8(14)	0.105 2	0.149(4)	0.199(6)
	4,4	0.019 0(31)	0.077 5	0.144(13)	0.192(22)
	5,5	0.008 7(56)			
6.0	2,2	0.062 7(3)	0.096 6	0.106 6(7)	0.121 7(9)
	3,3	0.030 3(10)	0.061 7	0.078 6(25)	0.090 2(29)
	4,4	0.015 5(21)	0.044 5	0.067 8(67)	0.078 9(77)
	5,5	0.008 2(37)	0.031 6	0.061 5(146)	0.072 2(183)
8.0	2,2	0.048 3(3)	0.069 0	0.074 0(6)	0.080 9(5)
	3,3	0.024 4(8)	0.043 1	0.049 9(19)	0.056 0(17)
	4,4	0.012 8(17)	0.030 7	0.040 5(49)	0.045 2(40)
	5,5	0.006 4(29)	0.021 8	0.038 8(108)	0.040 0(83)
10.0	2,2	0.039 1(3)	0.053 6	0.057 1(4)	0.060 9(4)
	3,3	0.020 3(8)	0.032 9	0.038 5(12)	0.040 8(15)
	4,4	0.011 5(16)	0.023 3	0.030 5(26)	0.032 3(34)
	5,5	0.006 3(33)	0.016 5	0.027 5(50)	0.028 0(67)
60.0	2,2	0.007 18(4)	0.008 02	0.008 35(4)	0.008 42(3)
	3,3	0.004 09(13)	0.004 64	0.004 93(11)	0.004 98(9)
	4,4	0.002 60(28)	0.003 17	0.003 42(25)	0.003 43(19)
	5,5	0.001 73(50)	0.002 25	0.002 64(44)	0.002 74(35)
	6,6	0.001 09(80)	0.001 53	0.001 98(71)	0.002 23(57)

Yotsuyanagi's,<sup>7</sup> show no evidence of quark confinement. However, to settle this question it would probably be necessary to measure very large loops because of the slow convergence of the time derivative (7.3) to the static potential (plus the self-energies). It might also be necessary to work at stronger coupling.

### XIII. RENORMALIZATION

Like any way of calculating quantities in field theory, the noncompact method requires renormalization. Because the method approximates ratios of the Euclidean path integrals of the continuum theory, its renormalization is similar to that of the continuum theory.

The ratio of multiple integrals (11.1) which is approximated by the noncompact method is the mean value in the bare vacuum of a product of the arbitrary operator  $Q(A)$  being evaluated, the projection operator  $\Pi_G$  on the subspace of gauge-invariant states, and the projection operator  $\Pi_V \equiv \lim_{t \rightarrow \infty} \exp(-tH)$  on the physical vacuum. Without any renormalization, the Hamiltonian  $H$  of the continuum theory, being a sum of squares of Hermitian field strengths  $F_{ij}^a$ , is positive and divergent. With the cutoff provided by the lattice spacing  $a$ , the  $H$  of the noncompact method is positive but too big. Since the probability distribution  $\exp[-S(A)]$  of the method essentially represents the exponential  $\exp(-tH)$ , this dis-

tribution is overly damped before renormalization. Thus the fluctuations of the fields are too damped. Since large Wilson loops are more sensitive to fluctuations than small ones, the Creutz ratios of the unrenormalized noncompact method are too small, as we have seen in the preceding section.

There is one instructive exception to this conclusion: namely, the case of the free field theory  $U(1)$  for which the unrenormalized Hamiltonian differs from the renormalized one merely by a divergent constant. In this case the probability distribution  $\exp[-S(A)]$  is overdamped by a constant factor, independent of  $A$ , which does not affect ratios such as (11.1). This is why the noncompact method without renormalization gives for  $U(1)_3$  the correct values of the Creutz ratios for arbitrary coupling.<sup>10</sup>

In a renormalizable theory, one may keep physical quantities finite while removing the cutoff either by subtracting counterterms or by redefining the constants in the unrenormalized Lagrangian. In a pure gauge theory, there are two adjustable constants, the coupling constant and the scale of the fields, apart from ones that refer to gauge fixing. Thus for  $SU(2)$  in the noncompact method, there are two parameters that we must adjust as the lattice spacing  $a$  tends to zero:  $Z_g$  and  $Z_A$ . Wilson loops are independent of  $Z_A$ , however, so to renormalize our computation of them, we need only adjust  $Z_g$  or equivalently the unrenormalized inverse coupling  $\beta_0$ .

Since there are no experiments in three-dimensional space-time, we have chosen to renormalize the noncompact method by comparing its Creutz ratios for small loops at weak coupling with those given by our perturbative formula. We have made such comparisons by using our Monte Carlo data at  $\beta_0=10$  and 60 and by varying in each case the value of  $\beta$  in our perturbative formula (9.5) until the 3-by-3 Creutz ratios matched. We denote such  $\beta$  as  $\beta(\beta_0)$ . We then examined how much the noncompact and perturbative Creutz ratios differed for smaller and larger loops. For  $\beta_0=10$ , we found  $\beta(10)=15$ . At  $\beta_0=10$  and  $\beta=15$ , respectively, the ratio  $\chi_{NC}(2a,2a)$  was 16% higher than  $\chi_P(2a,2a)$ , while  $\chi_{NC}(4a,4a)$  was 19% lower than  $\chi_P(4a,4a)$ . Now the perturbative formula is only valid when the size of the loop in lattice units  $\sqrt{(r/a)^2+(t/a)^2}$  is much less than  $1.8\beta$ . For the 4-by-4 loop at  $\beta=15$ , the former is 21% of the latter; so for that loop the formula is only marginally valid.

It was to avoid this theoretical uncertainty in the perturbative formula for  $\beta \leq 15$  that we also renormalized the noncompact method at  $\beta_0=60$ . We found  $\beta(60)=68$  for which value the formula is probably reliable even for the 5-by-5 loop and possibly for the 6-by-6 loop as well. At  $\beta_0=60$  and  $\beta=68$ , respectively, the ratio  $\chi_{NC}(2a,2a)$  was 1.4% higher than  $\chi_P(2a,2a)$ , while  $\chi_{NC}(4a,4a)$  was 6.9% lower than  $\chi_P(4a,4a)$ ,  $\chi_{NC}(5a,5a)$  was 12% lower than  $\chi_P(5a,5a)$ , and  $\chi_{NC}(6a,6a)$  was 19% lower than  $\chi_P(6a,6a)$ . As the size of the loop increases,  $\chi_{NC}$  falls off faster than  $\chi_P$ .

We have also renormalized the compact method using data at  $\beta_0=10$  and 60 from our simulations guided both by Wilson's action and by Manton's. For the case of Wilson's action we found  $\beta(10)=8.4$  and  $\beta(60)=56$ . At

$\beta_0=10$  and  $\beta=8.4$ , respectively, the ratio  $\chi_W(2a,2a)$  was 7.1% lower than  $\chi_P(2a,2a)$ , while  $\chi_W(4a,4a)$  was 11% higher than  $\chi_P(4a,4a)$ . At  $\beta_0=60$  and  $\beta=56$ , respectively, the ratio  $\chi_W(2a,2a)$  was 2.7% lower than  $\chi_P(2a,2a)$ , while  $\chi_W(4a,4a)$  was 1.8% higher than  $\chi_P(4a,4a)$ ,  $\chi_W(5a,5a)$  was 15% higher than  $\chi_P(5a,5a)$ , and  $\chi_W(6a,6a)$  was 35% higher than  $\chi_P(6a,6a)$ . As the size of the loop increases,  $\chi_W$  falls off slower than  $\chi_P$ .

For the case of Manton's action, we found  $\beta(10)=8.8$  and  $\beta(60)=57$ . At  $\beta_0=10$  and  $\beta=8.8$ , respectively, the ratio  $\chi_M(2a,2a)$  was 8.1% lower than  $\chi_P(2a,2a)$ , while  $\chi_M(4a,4a)$  was 11% higher than  $\chi_P(4a,4a)$ . At  $\beta_0=60$  and  $\beta=57$ , respectively, the ratio  $\chi_M(2a,2a)$  was 1.9% lower than  $\chi_P(2a,2a)$ ,  $\chi_M(4a,4a)$  was 1.3% higher than  $\chi_P(4a,4a)$ ,  $\chi_M(5a,5a)$  was 11% higher than  $\chi_P(5a,5a)$ , and  $\chi_M(6a,6a)$  was 22% higher than  $\chi_P(6a,6a)$ . As the size of the loop increases,  $\chi_M$  falls off slower than  $\chi_P$ .

Despite the marginal accuracy of the perturbative formula and of the data in some of these comparisons, there is a trend that is so consistent as to be probably true: the forces predicted by the noncompact method fall off faster with distance than those of the perturbative formula, while those of the compact method fall off slower than both.

Cornwall, Hou, and King have found approximate nonperturbative solutions to the Schwinger-Dyson equation for a version of the gauge propagator corresponding to an infinite set of Feynman diagrams.<sup>29</sup> Their solutions avoid the tachyonic pole (4.2) and exhibit dynamically generated masses,  $m = 15c_A \xi g^2 / (32\pi)$  for  $\xi$  greater than about 1.96. The forces predicted by their propagator presumably fall off faster with distance than those of the perturbative formula, in agreement with the noncompact method.

In our noncompact simulations, however, we measured correlations of spatially separated  $a$ -by- $a$  Wilson loops and found a value for the gluon mass that was consistent with zero. But Nešić found  $m \sim 0.4g/a$  by measuring the transverse gluon propagator.<sup>8</sup>

#### XIV. SUMMARY AND CONCLUSIONS

We have described and applied to  $SU(2)_3$  a Monte Carlo method that directly approximates the ratios of Euclidean path integrals that occur in continuum gauge theories. The basic variables of this "noncompact" method are fields rather than elements of a gauge group as in Wilson's "compact" method. This noncompact method uses the continuum action, may be closer to the exact theory, and does not have confinement trivially built in.

The compact method has an exact lattice gauge symmetry that approximates the gauge invariance of the continuum theory. But it achieves this exact lattice symmetry by compromising the continuum fields and action, quantities that are respected in the noncompact method. The noncompact method functionally integrates over linearly interpolated fields and gives the correct weight  $e^{-S(A)}$  to each such field  $A$ , where  $S(A)$  is the exact gauge-invariant, continuum action of the field  $A$ . Because the space of linearly interpolated fields is gauge invariant only in the continuum limit in which it becomes

dense in the space of all continuous fields, it is not clear which side of this trade-off is more accurate for non-Abelian theories.

To provide a standard against which to compare the results of both compact and noncompact simulations, we have derived in continuum perturbation theory a formula for Wilson loops in three dimensions valid to fourth order in the coupling constant for any compact, semisimple Lie group. We have also developed a version of the formula that incorporates a correction for periodic boundary conditions.

We have presented a critique of compact lattice gauge theory, describing four approximations that collectively cause compact lattice actions to be globally different from the Yang-Mills action. As a result of this difference, the distribution of the Yang-Mills action per plaquette in compact simulations is broader and shifted to larger values than that of the guiding compact action. The links of compact simulations thus are less correlated than those of simulations guided by the Yang-Mills action.

We have measured Creutz ratios of Wilson loops in noncompact simulations and in compact simulations both guided by Wilson's action and by Manton's. Before renormalization the Wilson loops of the noncompact simulations fall off slower than those of the compact simulations as the area of the loop increases. Before renormalization the Creutz ratios of the noncompact method are smaller than those of the perturbative formula, while those obtained with Manton's action are larger than the perturbative ratios, and those with Wilson's action still larger. Although some of these differences can be absorbed by the renormalization of the two methods, the following trend remains: the forces predicted by the noncompact method fall off faster with distance than those of the perturbative formula, while those of the compact method fall off slower. The noncompact simulations

show no evidence of quark confinement.

We have offered evidence that suggests that the confinement signal in compact lattice gauge theory may be an artifact of that method. This evidence is not compelling, however, for various reasons: our work was in three rather than four space-time dimensions; it was done on a  $16^3$  lattice, rather than on a much larger one; and our noncompact method may have flaws. Yet our preliminary noncompact simulations of SU(2) in four dimensions as well as those of other groups<sup>5,6</sup> also show no sign of confinement. Perhaps the most interesting theoretical interpretation of our findings is provided by recent work of Gribov's<sup>4</sup> in which he argued that confinement occurs only in QCD with quarks that are light compared to the strong-interaction scale  $\Lambda$  and not in pure or heavy-quark QCD.

#### ACKNOWLEDGMENTS

We are grateful to M. Creutz, U. Heller, and S. Otto for sending us their programs and for advice, and to J. Banks, E. Brézin, G. Cahill, C. Chandler, D. Clarke, S. Coleman, J. Cornwall, N. Duric, E. Esau, R. Glauber, M. Grady, S. Gregory, V. N. Gribov, P. Hasenfratz, M. Hebert, J. Jersák, J. King, J. Mandula, B. Moussallam, D. Nešić, C. Rebbi, R. Reeder, B. Richert, E. Seiler, J. Smit, I. Stamatescu, and D. Zwanziger for useful conversations. K.C. would like to thank Professor Frank Pipkin for his hospitality during a sabbatical year at Harvard. The computations of this paper were done by a Ridge 32C at UNM, an IBM 3090 in Lyon, and a Cray X-MP at the National Magnetic-Fusion Energy Computing Center. This research was supported by the Department of Energy under Grant No. DE-FG04-84ER40166 and by Sandia National Laboratories under a Sandia-University Research Program grant, and was partly done at the Aspen Center for Physics.

\*Permanent address.

<sup>1</sup>K. Wilson, Phys. Rev. D **10**, 2445 (1974).

<sup>2</sup>M. Creutz, Phys. Rev. Lett. **45**, 313 (1980).

<sup>3</sup>M. Creutz and K. Moriarty, Phys. Rev. D **26**, 2166 (1982).

<sup>4</sup>V. N. Gribov, Phys. Scr. **T15**, 164 (1987); Phys. Lett. B **194**, 119 (1987).

<sup>5</sup>A. Patrascioiu, E. Seiler, and I. Stamatescu, Phys. Lett. **107B**, 364 (1981).

<sup>6</sup>E. Seiler, I. Stamatescu, and D. Zwanziger, Nucl. Phys. **B239**, 177 (1984); **239**, 201 (1984).

<sup>7</sup>I. Yotsuyanagi, Phys. Lett. **135B**, 140 (1984).

<sup>8</sup>D. Nešić, New York University Report No. NYU/TR1/85 (unpublished); Ph.D. thesis, New York University, 1985.

<sup>9</sup>K. Cahill, S. Prasad, and R. Reeder, Phys. Lett. **149B**, 377 (1984).

<sup>10</sup>K. Cahill and R. Reeder, Phys. Lett. **168B**, 381 (1986); J. Stat. Phys. **43**, 1043 (1986).

<sup>11</sup>K. Cahill and R. Reeder, *Advances in Lattice Gauge Theory* (World Scientific, Singapore, 1985), p. 424.

<sup>12</sup>K. Cahill, S. Prasad, R. Reeder, and B. Richert, Phys. Lett. B **181**, 333 (1986).

<sup>13</sup>K. Cahill, M. Hebert, and S. Prasad, Phys. Lett. B **210**, 198 (1988).

<sup>14</sup>N. Manton, Phys. Lett. **96B**, 328 (1980).

<sup>15</sup>K. Cahill and D. Stump, Phys. Rev. D **20**, 2096 (1979).

<sup>16</sup>R. Jackiw and S. Templeton, Phys. Rev. D **23**, 2291 (1981).

<sup>17</sup>T. Appelquist and R. Pisarski, Phys. Rev. D **23**, 2305 (1981).

<sup>18</sup>C. Lang, C. Rebbi, P. Salomonson, and B. Skagerstam, Phys. Lett. **101B**, 173 (1981).

<sup>19</sup>A. Hasenfratz and P. Hasenfratz, Phys. Lett. **93B**, 165 (1980); R. Dashen and D. Gross, Phys. Rev. D **23**, 2340 (1981).

<sup>20</sup>G. Mack and E. Pietarinen, Nucl. Phys. **B205**, 141 (1982).

<sup>21</sup>M. Grady, Z. Phys. C **39**, 125 (1988).

<sup>22</sup>H. Georgi, *Lie Algebras in Particle Physics* (Benjamin/Cummings, Reading, MA, 1982), p. 115.

<sup>23</sup>V. N. Gribov, Nucl. Phys. **B192**, 1 (1978).

<sup>24</sup>J. Banks and K. Cahill (unpublished).

<sup>25</sup>M. Grady, SUNY-Fredonia Report No. SUNYFRED/8802 (unpublished).

<sup>26</sup>A. Patrascioiu, E. Seiler, V. Linke, and I. Stamatescu, Max-Planck-Institut Report No. MPI-PAE/PTh 51/88 (unpublished).

<sup>27</sup>M. Creutz, Phys. Rev. D **21**, 2308 (1980).

<sup>28</sup>E. D'Hoker, Nucl. Phys. **B180**, 341 (1981); J. Ambjørn, A. Hey, and S. Otto, *ibid.* **B210**, 347 (1982); J. Ambjørn, P. Olesen, and C. Peterson, *ibid.* **B244**, 262 (1984).

<sup>29</sup>J. Cornwall, Phys. Rev. D **26**, 1453 (1982); J. Cornwall, W.-S. Hou, and J. King, Phys. Lett. **153B**, 173 (1985).